Journal of Engineering Science *Vol. XXVII, no. 3 (2020), pp. 111 - 133*
Fascicle *Electronics and Computer Science* *ISSN 2587-3474*
Topic *Computers and Information Technology* *eISSN 2587-3482*

DOI: 10.5281/zenodo.3949678
UDC 004.7

APPROXIMATE MAIN VALUE PERFORMANCE ANALYSIS OF COMPUTING PROCESS USING SHPN WITH FUZZY PARAMETERS

Emilian Guțuleac*, ORCID ID: 0000-0001-6839-514X,
Sergiu Zaporojan, ORCID ID: 0000-0001-5928-4229,
Victor Moraru, ORCID ID: 0000-0002-5454-8341,
Alexei Sclifos, ORCID ID: 0000-0003-4531-7944,
Andrei Furtună, ORCID ID: 0000-0003-0057-2407

Technical University of Moldova, 168 Stefan cel Mare bvd., MD-2004 Chisinau, Republic of Moldova
*Corresponding author: Emilian Guțuleac, *emilian.gutuleac@calc.utm.md*

Received: 04. 28. 2020
Accepted: 06. 12. 2020

Abstract. Stochastic fluid models are a class of analytic models that have recently drawn the attention of many researchers for the modeling and performance evaluation of complex computer systems and networks (CSN). In this paper we present an approximated main-value analysis method of stochastic hybrid Petri nets (SHPN) models with fuzzy parameters (FSHPN) for performances evaluation of data continuous transmission CSN virtual channels. The method is based on the main-value analytical solution of one buffer finite FSHPN sub-models, also referred dipoles as building blocks. We develop a fixed point iterative algorithm to accurately estimate performance measures of buffer pipe-line FSHPN models such as throughput and mean buffer contents. The accuracy of the proposed method has been validated by simulation experiments.

Keywords: *aggregation, approximation, computer system and networks, decomposition, evaluation, fuzzy numbers, hybrid, Petri nets, stochastic, throughput.*

1. Introduction

Formal modeling and techniques for performance evaluation and dependability measures are widely used while designing and analyzing many types of computer systems and computer networks (CSN) with discrete-continuous process applications, based on which design gaps can be identified at the early stage of their life cycle [1, 2]. As a result, these issues can be eliminated earlier and the costs of troubleshooting and maintenance can be significantly reduced.

The development of appropriate models is crucial for the design, performance and dependability analysis and control of dynamic CSN. The usefulness of a model depends on both its capacity to capture the relevant features of the system, and its capacity for mathematical analysis. These capacities of the model largely rely on the adopted modeling formalism, i.e. on the set of modeling principles and rules that are used to build the model. Also, randomness and uncertainty are two major problems one faces while modeling

nonlinear dynamics of CSN. Stochastic and fuzzy methods are used to cope with these problems [3].

Among the most popular modeling formalisms, due to the advantage of quick construction and numerical analysis, extended Petri net (PN) [4], such as generalized stochastic Petri nets (GSPN) [5] and stochastic reward nets (SRN) [6] formalisms, are recognized paradigms for performance and dependability analysis of various systems such as distributed computing network, network communication protocols, industrial systems etc. In addition, analytical modeling using these formalisms is a less costly and more efficient method compared to simulation techniques [2]. It generally provides the best insight into the effects of various parameters and their interactions. With respect to other more popular techniques of graphical system representation, these formalisms are particularly suited to represent in natural way logical interactions among parts or activities in a system. Typical situations that can be modeled by PN are synchronization, sequentially, concurrency conflict, etc. Also, some advantages of GSPNs and SRNs are that they allow graphical editing of the model, they are easy to understand, they are powerful and flexible, and they can be simulated automatically by a computer.

Despite the existence of an impressive amount of results in the literature for the analysis of GSPNs and SRNs models, many analysis techniques cannot be applied to large systems due to the so called *state explosion problem* (i.e., the set of reachable markings increases exponentially) [5, 6]. *For this reason*, the *fluidification* (i.e., getting continuous-state approximations) has been proposed as a relaxation technique that overcomes the state explosion problem by introducing *fluid stochastic Petri nets* (FSPN) [7] and *stochastic hybrid Petri nets* (SHPN) [8, 9]. The idea consists in the analysis of the GSPN or SRN models via a relaxed continuous version, reducing thus the computationnal efforts and, at the same time, hoping that the information obtained from the continuous model be valid for the original discrete one.

Moreover, uncertainty handling is a central topic in performance and dependability analysis of CSN. The task of CSN modeling and analysis is often hampered by the lack of detailed system parameter information, a limited knowledge of the system behavior to be modeled and the difficulty of obtaining accurate data. This often results in a number of uncertain system parameters that need to be incorporated into a mathematical model. Although, the most common approach used to represent uncertainty in modeling systems are based on stochastic process theory, such models are not always suitable to describe all dimensions of uncertainty. Especially the inaccuracy of data which, for example, is the result of limited measurement accuracy which is not statistical in nature and cannot be described using probability measures [3]. Meanwhile, uncertainty in many CSN performance and dependability modeling is unavoidable. Hence, to deal with uncertain information in stochastic models, the fuzzy set theory [10, 11] and the concept of fuzzy numbers is well suited to use for handling vague conditions that include behavior uncertainties and parameter inaccuracies.

GSPN, SRN, FSPN and SHPN formalisms assume the availability of cert values of quantitative parameters. To deal with uncertainty the GSPN with fuzzy parameters approaches have been proposed in papers [10]. In these approaches, the transition firing rates as well as states probabilities can be considered as fuzzy numbers.

In this context, it is necessary to enhance the FSPN and SHPN formalisms with fuzzy parameters that will allow adapting all available data, even if they are uncertain, to use and

build useful models. Although, FSPNs and SHPNs are prominent formalisms applied for modeling and performance evaluation of hybrid dynamic systems with discrete and continuous components, that interact with each other, an analytical evaluation of the performance measures of these models requires the solution of a complex first-order hyperbolic partial differential equations, combined with boundary algebraic equations, whose numerical analysis becomes a very difficult task [3].

An FSPNs or SHPN model of a hybrid sistem with $N \geq 4$ continuous places (buffers) cannot be accurately analyzed analytically [7, 9, 12], thus justifying the development of approximation methods for analysis of these types models.

To tackle this issue, in this paper, we present a decomposition mean-value analytical method for approximate performance analysis of continuous data transmission network virtual channel, modeled by SHPN with fuzzy parameters and finite capacity buffers. The basic idea is the following: the overall SHPN model is decoupled into simpler and more tractable SHPN sub-models. We uses the mean-value analytical solution of two-stage SHPN sub-model with one buffer as a building block, called dipole, and the performance measures obtained from the solution of the sub-models are then used to compute those concerning the overall model. In order to take into account the propagating effect of partial and complete blocking and starvation phenomena of servers throughout the system, analytical decomposition expressions for iterative modification parameters of each dipole are provided similarly as proposed in [13, 14]. Based on this method, a *fixed point iterative procedure* for efficient estimation, with a given accuracy, of the performance measures of a SHPN with fuzzy parameters and pipe – line finite capacity buffers is developed. Numerical results and simulation prove the good accuracy of the developed method.

2. Stochastic hybrid petri nets with fuzzy parameters

2.1. Elements of fuzzy sets theory and fuzzy numbers

The fuzzy sets theory (FST) and concepts with fuzzy numbers [15] appears from the need to deal with imprecise, vague or partially true information to exact values but the range of possible values are known. In classical set theory, membership of an element in a set is considered to be binary. However, FST allows an element of a set to have a membership value from the interval [0, 1]. To facilitate the exposition of the proposed approach, in this subsection we present some basic elements of fuzzy sets, triangular fuzzy numbers (TFN) and arithmetic algebraic operations according to [15], required for defining SHPNs with fuzzy parameters.

A fuzzy subset $\widetilde{A}$ of of the set of real numbers IR is defined by its membership function $\mu_{\widetilde{A}} : I\widetilde{R} \to [0,1]$, which assigns a real number $\mu_{\widetilde{A}}$ in the interval $[0,1]$ to each element $\widetilde{x} \in I\widetilde{R}$, where the value of $\mu_{\widetilde{A}}$ at x shows the grade of membership of x in $\widetilde{A}$.

A fuzzy number is a fuzzy set $\widetilde{a} : IR \to [0,1]$ which satisfies: 1) $\widetilde{a}$ is upper semicontinuous; 2) $\widetilde{a}(x)$ outside some interval $[0,1]$; 3) there are real numbers a, b in $[c, d]$ for which: (*i*) $\widetilde{a}(x)$ is monotonic increasing on $[c, a]$; (*ii*) $\widetilde{a}(x)$ is monotonic decreasing on $[b, d]$; (*iii*) $\widetilde{a}(x) = 1$, for $a \leq x \leq b$. Fuzzy numbers can be considered from two different points of view: with their membership function or with their α-cuts. The two ways of considering fuzzy numbers are equivalent, and, depending on the details we want to study, one can be better than the other.

In this paper, we consider a fuzzy number in the form of $\tilde{a} = (a, \delta, \beta)$, where a is the *center*, δ is the *left width*, and β is the *right width*. For arbitrary fuzzy number $\tilde{a} = (a, \delta, \beta)$, the membership function is of the following form:

$$\mu_{\tilde{a}}(x) = \begin{cases} 1-(a-x)/\delta, & a-\delta \le x \le a, \\ 1-(x-a)/\beta, & a \le x \le a+\beta, \\ 0, & otherwise. \end{cases}$$

On the other hand, a parametric $\alpha - cut$ fuzzy number $\tilde{a} = [a^-(\alpha), a^+(\alpha)]$ can be represented as: $a^-(\alpha) = a-(1-\alpha)\delta$ and $a^+(\alpha) = a+(1-\alpha)\beta$.

Two type's of fuzzy numbers are most commonly found in real applications: trapezoidal fuzzy numbers and triangular fuzzy numbers (TFN). The use of these types fuzzy numbers is more appropriate, one reason being the computing complexity. Between these, TFN are often used because the computation is simplified and the results are easier interpreted and implemented.

The arithmetic algebraic operations for TFN $\tilde{a} = (a, \delta, \beta)$ and $\tilde{b} = (b, \gamma, \varepsilon)$ numbers are as follows [15]: 1) *Addition* $\tilde{c} = \tilde{a} \oplus \tilde{b} = (a+b, \delta+\gamma, \beta+\varepsilon)$; 2) *Subtraction* $\tilde{c} = \tilde{a} \varnothing \tilde{b} = (a-b, \delta+\varepsilon, \beta+\gamma)$; 3) *Multiplication* $\tilde{a}$ positive with $\tilde{b}$ positive $\tilde{c} = \tilde{a} \otimes \tilde{b} = (a \cdot b, a \cdot \gamma + b \cdot \delta, a \cdot \varepsilon + b \cdot \beta)$; 4) *Scalar product*: $\tilde{c} = \kappa \otimes \tilde{a} = (\kappa \cdot a, \kappa \cdot \delta, \kappa \cdot \beta), \kappa \ge 0.$

The *inverse* for triangular fuzzy number is: $\tilde{c} = 1/\tilde{a} = \left(1/a, \beta/a^2, \delta/a^2\right).$

2.2. Basic concepts and elements of SHPN with fuzzy parameters

We assume that the readers are familiar with the basic concepts of $GSPN$, $FSPN$ or $SHPN$. A comprehensive theoretical treatment of these topics is outside the scope of this paper. For more comprehensive details to $SHPN$ we let the readers refer to [8, 9]. In this section we provide a brief presentation of the $SHPN$ with fuzzy parameters, called $FSHPN$.

Let IN_+ be the set of nonnegative integers, and IR_+ is the set of positive real numbers.

The particularities of the $SHPN$, underlying of $FSHPN$, consist in the fact that both the set P of places constitutes a partition $P = P_d \cup P_c$, $P_d \cap P_c = \varnothing$, where P_d is the set of discrete places and P_c is the set of continuous places (buffers), which can have a finite capacity. The set T of timed transitions constitutes a partition $T = T_d \cup T_c$, $T_d \cap T_c = \varnothing$, where T_d is the set of discrete transitions T_c and is the set of continuous transitions. The discrete places p_k can contain an integer number of tokens, and the continuous places can contain an real quantity of fluid. The discrete places graphically are represented by simple circles, and the continuous ones by two concentric circles. The set of discrete transitions T_d in turn is partitioned into a subset of *timed* transitions T_τ (resp. immediate T_0), $T_d = T_\tau \cup T_0$, $T_\tau \cap T_0 = \varnothing$, which are represented by *thick* black bars (resp. *thin* black bars), and the continuous ones are represented by small rectangles. A positive integer marking-dependent priority function $\Pr i(t_j) \in IN_+$ is associated with each one transition $t_j \in T_d$ for which $\Pr i(T_0) > \Pr i(T_\tau)$. Also, with each transition $t_j \in T$, a guard function $g(t_j) \in T$ is associated, which is a marking-

dependent Boolean function, that condition the enabling and selection of the triggering of these transitions.

The current marking $(M,\vec{x})$ of $SHPN$ is a column vector that shows respectively the common distribution of tokens in discrete places and fluid levels in buffers. The discrete part of this marking M is represented by the column vector containing a positive integer number of tokens $m_n = M(p_n)$ in the discrete places p_n, and $\vec{x}$ is the continuous marking column vector of the buffers b_i in which it represents the fluid level in the buffers, which are a real positive quantites. Each b_i has a maximum storage capacity $h_i \in IR_+$ of the respective fluid. The discrete tokens are consumed and produced in accordance with the rules for triggering enabled discrete transitions through normal discrete arcs. The continuous fluid flows are consumed and produced in accordance with the firing rules of enabled continuous transitions through normal fluid arcs or fluid setting arcs [8]. So, when the respective continuous transition $u_k \in T_c$ is enabled, it continuously change the *fluid* level x_i of the incident buffers with speed $v_k(M,\vec{x}) \in IR_+$.

The graphical representation of all $SHPN$ primitives is given in Figure 1

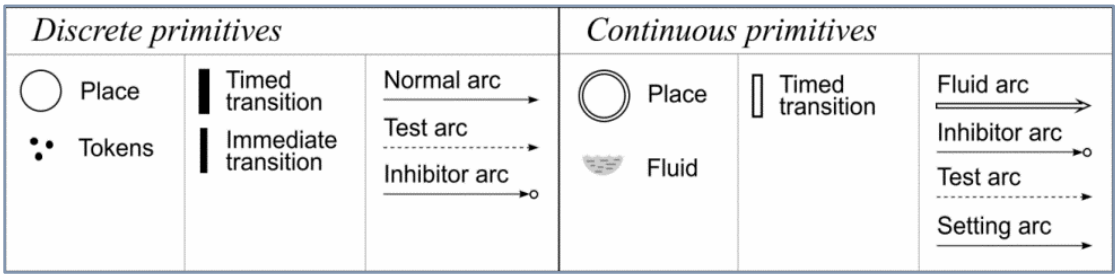

Figure 1. All primitives of a $SHPN$ models.

Inhibitory arcs (resp. *test arcs*) *disable* (resp. *activate*) a transition when a certain number of tokens or a certain amount of fluid is present in a discrete or continuous place, respectively.

The firing delay of timed discrete transitions $t_l \in T_\tau$ are defined by firing fuzzy rates $\lambda_l(M,\vec{x}) \in IR_+$, which may depend on the current marking of $SHPN$. With the immediate discrete transitions $t_j \in T_0$ are associated fuzzy weights $w_j(M,\vec{x}) \in IR_+$, based on which their firing fuzzy probabilities are calculated. The fluid content in buffers is changed either by continuous transitions u_k depending on their firing fuzzy speed, which may depend on the current discrete marking of the $SHPN$, that it can be directly established by a setting cardinality of arcs at a certain value, when a discrete transition will be fired.

Figure 2 shows the possible connections between discrete and continuous places with a discrete (resp. continuous) transition through different types of arcs.

The detailed definition of the $SHPN$, its quantitative attributes, the enabling and firing rules of the respective transitions by the current marking are presented in [8, 9].

A $FSHPN$ model is described by a underlyng $SHPN$ in which its parameters $\tilde{\lambda}_l(M,\vec{x})$, $w_j(M,\vec{x})$ and $v_k(M,\vec{x})$ are the respective fuzzy numbers [10, 15]. These fuzzy parameters of $FSHPN$ are noted in the following: $\tilde{\lambda}_l(M,\vec{x}), w_j(M,\vec{x})$ and $\tilde{v}_k(M,\vec{x})$.

Modelling complex CSN using $FSHPN$ network models allows us to better understand their behaviour, to estimate and ultimately to improve their performance.

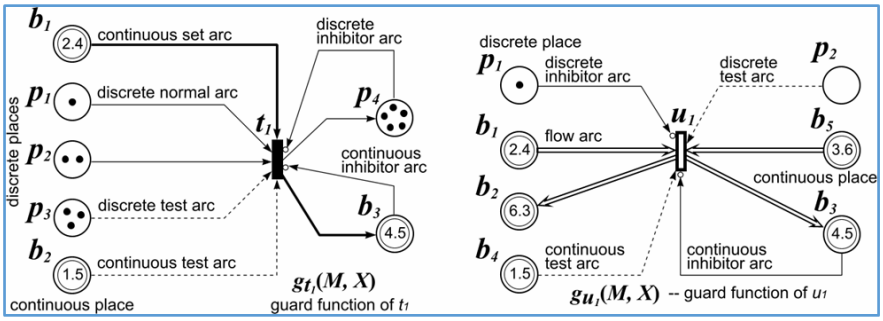

Figure 2. The posible connections between discrete and continuous places with discrete or transitions through different types of arcs.

Due to the restriction space for the presentation of proposed method in this paper, we will limit to the fact that only one buffer is incident forward (resp. backward) to the continuous transi-tions of an $FSHPN$ model, i. e. $|{}^{\bullet}u_i|=1$ and/or $|u_i^{\bullet}|=1$ [8]. Also, we consider the $FSHPN$ models whose continuous markings have no influence to the discrete ones, i.e. every discrete marking determines completely both the set of enabled transitions, their firing rates and the fluid flow speeds of the incoming and outgoing arcs for each buffers.

3. Approximate mean-value performance analysis method of continuous flow pipe-line discrete - computing process with $FSHPN$

3.1. Modeling of continuous data transmission network virtual channel with $FSHPN$

To present the method of approximate mean-value performance analysis of pipe-line discrete-continuous computing process with $FSHPN$ models we will consider a virtual channel of computer network (VCN) [16 -19] for continuous pipe-line transmission data flow consisting of N node, called servers $Sv_1, Sv_2, \cdots, Sv_N$, and $N-1$ buffers $b_1, b_2, \cdots, b_{N-1}$. Each Sv_i interacts and cooperates with each other through a continuous data storage buffer b_i with a storage capacity h_i [8]. Figure 1 shows such a virtual channel of a computer network.

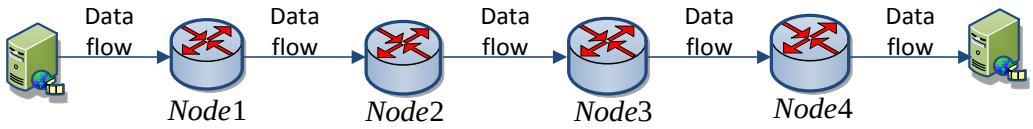

Figure 3. A virtual channel of computer network.

Modeling assumptions of an VCN *with* $FSHPN$. The construction of the model of VCN in the form of $FSHPN$ is based on the adoption of the following hypotheses: 1) It is considered that the data flow that processed and transmitted by VCN is continuous, interpreted as fluid; 2) The data flow enters to the server Sv_i is being processedin *active state* and stored in the buffer b_i with a finite capacity h_i, then from this buffer it passes to the server Sv_{i+1} and finally from the server Sv_N it leaves the system; 3) When a server Sv_i goes into the *passive state* (for example, it is faulty) in a certain way, it does not process and transmit the data flow; 4) The first server Sv_1 is never starved and the last one Sv_N is *never blocked*; 4) Servers Sv_i have different data flow processing speeds $\tilde{v}_{i,l}$; 5) In the initial state, all the servers are operational (they are in *active states*); 6) At the same time a server cannot be in

more than one passive state (failure modes). Even if a server that is in a given failure mode cannot fail in another way before it is repaired; 7) The respective rates of change of the discrete local states follow exponential distributions. 8) The discrete part of $FSHPN$ is *bounded*, *live* and *reversible*, i.e. it underlying $FGSPN$ has a stationary regime [8, 9].

In these modeling assumptions the behavior of such a VCN is as follows. Suppose the server Sv_2 is in a *passive state*, and the other servers are still functional i.e. in *active states* (see Figure 4). This causes the amount x_2 of fluid to decrease in the buffer b_2 while the amount x_1 of fluid in the buffer b_1 increases. After the buffer b_2 is empty, the server Sv_3 will be starved. On the other hand, after the buffer b_1 is full, the server Sv_1 will be blocked. Moreover, it is also possible for servers to change the active state to a passive state. As an example, suppose the servers Sv_1 and Sv_2 are also functional. Suppose the server Sv_2 is running faster than the server Sv_1. When the buffer between these servers is empty, the server Sv_2 will slow down processing and run at the same speed as the server Sv_1. The case when the server Sv_1 is running faster than the server Sv_2 is similar. When all the servers can be either in passive or active state and they operate at different speeds, the throughput of this pipe-line system depends on the rate of change of states, the duration of presence in the passive or active states and the processing speed of the fluid by the servers. An illustration of the dynamic behavior of this type of VCN is given in Figure 4.

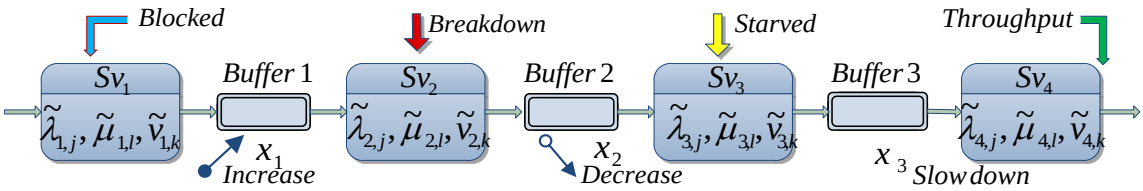

Figure 4. An illustration of the dynamic of data flow transmission through VCN.

Next, for the convenience of presenting and analyzing the $FSHPN$ models that describe the behavior of Sv_i, we will use the notations of the attributes of these models rendered by respective symbols that have two indices: the first index i indicates the number of order of belonging to the submodel $FSHPN_i$ that describes the behavior of Sv_i, and the second index indicates the order number of an attribute that belongs to this submodel, for example, discrete place $p_{i,k}$, discrete transition $t_{i,j}$ or continuous transition $u_{i,l}$, etc.

Figure 5 shows an example of a $FSHPN1$ model that describes the behavior of a VCN with $N=3$ servers and 2 buffers. The discrete part of $FSHPN1$ describes the algorithm for controlling the behavior of the continuous part of data flows processing.

In the model $FSHPN1$ shows in Figure 5, the notations used to list the discrete places, the discrete and continuous transitions have the following meanings:

$$pi\_k = p_{i,k},\ k=1,\cdots,8;\ \ ti\_j = t_{i,j},\ \ j=1,\cdots,8 \ \text{ and } \ ui\_l = t_{i,l},\ l=1,2.$$

The nominal fuzzy speeds $\tilde{v}_{i,l}$ of continuous data processing are associated with the respective continuous transitions $u_{i,l}$, and the fuzzy rates $\tilde{\lambda}_{i,j}(M)$ change of the discrete part states (for example, *failure* or *repair*; *active* or *passive*; *available* or *unavailable*) are respectively associated with the discrete timed transitions $t_{i,j}$. The respective local active

or passive state of Sv_i is shown by marking $m_{i,k} = M(p_{i,k}) = 1,\ k = 1, \cdots, k_d$ of discrete places $p_{i,k}$.

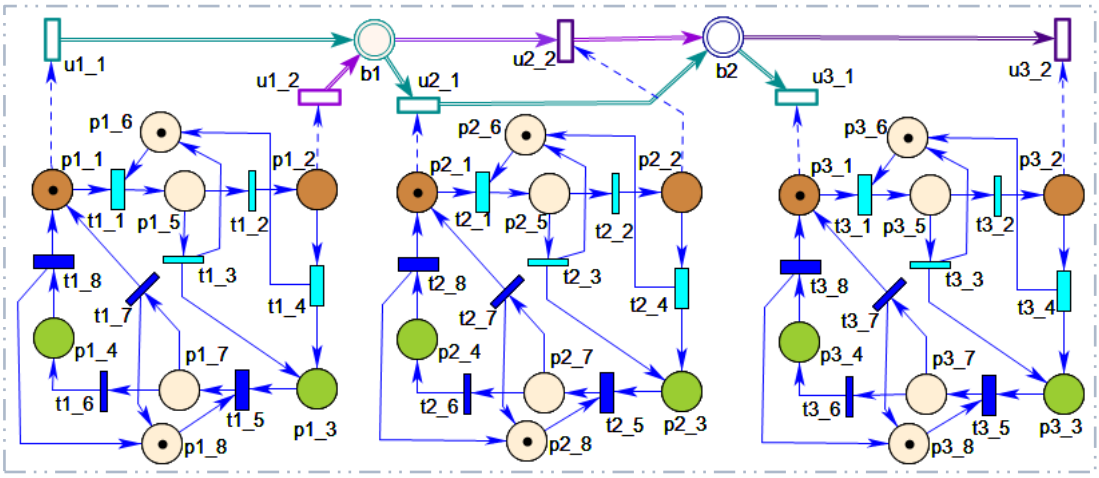

Figure 5. Example of $FSHPN1$ model of a VCN with 3 servers and 2 buffers.

As already mentioned, a model $FSPN$, $SHPN$ and also $FSHPN$ that has $N \geq 4$ buffers *cannot be accurately analyzed analytically* [9, 12], we will further develop a method of mean-value aggregate decomposition and approximation of the average performance measures of VCN and the distribution of the average content of buffers.

The proposed method was inspired by the studies of the production lines presented in the works [13 - 15]. For this we decompose VCN into $N-1$ *producer-consumer subsystems* DP_i, called *dipoles*. Each dipole DP_i consists of a SA_i fluid-producing server in the buffer b_i and a SD_i fluid-consuming server from the buffer b_i between these servers.

Figure 6 shows such an dipole DP_i of VCN whose behavior is presented in Figure 4.

In order to evaluate the performance of each dipole DP_i and then of the entire VCN system, we will build the aggregate model $FSHPN_{Svi}$ of each server Sv_i and also the model $FSHPN_i$ of each dipole DP_i.

Figure 7 shows the model $FSHPN1_i$ of such dipole DP_i of the virtual channel described by the model $FSHPN1$ presented in Figure 5.

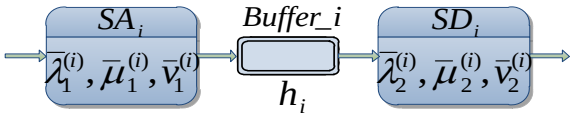

Figure 6. Dipole DP_i of a VCN whose behavior is shown in Figure 4.

Next, for the convenience of presentation, exposing and interpreting the behaviour of the $FSHPN1_i$ model of a dipole DP_i in Figure 7, for *upstream* (*producer*) $SA_i = Sv_i$ at the buffer b_i we will use the following notations of discrete places, discrete and continuous transitions: $pAi\_k = p_{i,k},\ k = 1, \cdots, 8$; $tAi\_j = t_{i,j},\ j = 1, \cdots, 8$; and $uAi\_l = t_{i,l},\ l = 1, 2$, and for *downstream* (*consumer*) $SD_i = Sv_{i+1}$ at the buffer b_i we will use the following notations: $pAi\_k = p_{i,k},\ k = 1, \cdots, 8$; $tAi\_j = t_{i,j},\ j = 1, \cdots, 8$; and, $uAi\_l = t_{i,l},\ l = 1, 2$.

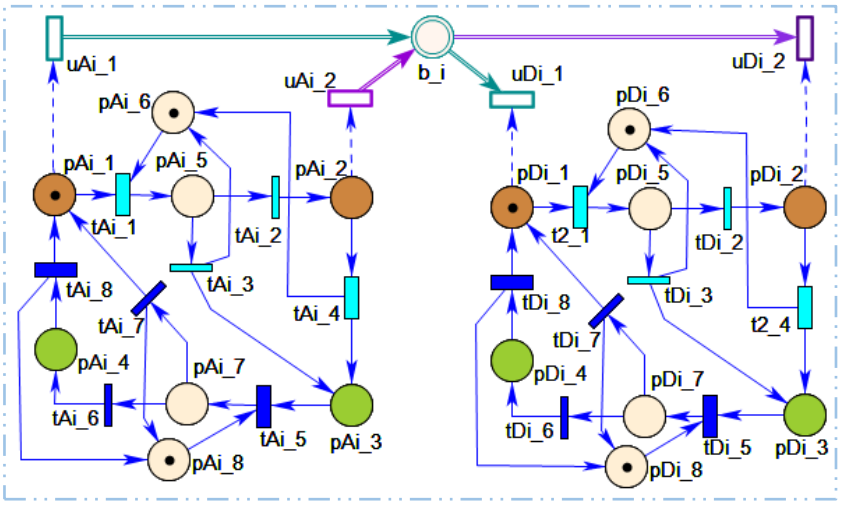

Figure 7. The model $FSHPN1_i$ of a dipole DP_i of $FSHPN1$ shown in figure 5.

3.2. Aggregate $FSHPN$ model of a dipole

As an example, the aggregate $FSHPN2_i$ model of a dipole DP_i, described by the model $FSHPN1_i$ in Figure 7, is shown in Figure 8. In this model, the aggregate quantitative fuzzy parameters are determined based on the fuzzy steady state probabilities $\tilde{\pi}_{i,k}$ of presence in the respective accessible markings $M_{i,k}$ of $FGSPN_{Svi}$ that describe the behavior of the discrete part $FSGPN_{Svi}$ of analyzed model $FSHPN_{Svi}$.

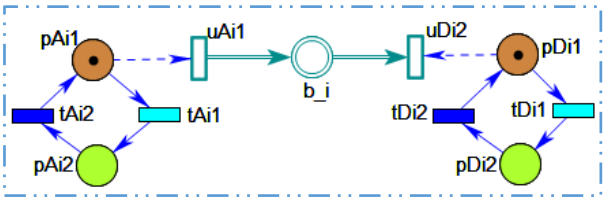

Figure 8. The aggregate model $FSHPN2_i$ of a dipole DP_i.

To specify and determine the values of the quantitative fuzzy parameters of the aggregate model $SHPN2_i$, for the upstream (producer) Sv_i at the buffer $b\_i = b_i$ we use the notations: $pAi1 = p_1^i$, $pAi2 = p_2^i$, $tAi1 = t_1^i$, $tAi2 = t_2^i$ and $uAi1 = u_1^i$, again for the downstream (consumer) Sv_{i+1} at the buffer $b\_i = b_i$ we use the notations: $pDi1 = p_1^{i+1}$, $pDi2 = p_2^{i+1}$, $tDi1 = t_1^{i+1}$, $tDi2 = t_2^{i+1}$ and $uDi1 = u_2^i$. *The meanings of discrete places*: p_1^i (resp. p_1^{i+1}) - is respectively the *active local state* in which Sv_i (resp. Sv_{i+1}) *produces* (resp. *consumes*) fluid with the aggregate speed $\bar{v}_1^{(i)}$ (resp. $\bar{v}_2^{(i)}$) *in* (resp. *from*) the buffer b_i, and p_2^i (resp. p_2^{i+1}) - is respectively the *passive local state* in which (resp.) does *not produce* (resp. *does not consume*) fluid *in* (resp. *from*) the buffer b_i. *The meanings of the discrete transitions*: t_1^i (resp. t_1^{i+1}) - represents respectively the activity in which Sv_i (resp. Sv_{i+1}) changes its *active* state into the *passive* one with the *aggregate rate* $\bar{\lambda}_1^{(i)}$ (resp. $\bar{\lambda}_2^{(i)}$), and t_2^i (resp. t_2^{i+1}) - represents respectively the activity in which Sv_i (resp. Sv_{i+1}) changes the *passive* state in the *active* one with the *aggregate rate* $\mu_1^{(i)}$ (resp. $\mu_2^{(i)}$).

The fully linear system of Chapman-Kolmogorov equations (FFLSE), that describes the continuous time Markov chaine (CTMC) behaviour of discrete part $FGSPN_{Svi}$ model of server Sv_i, is generated using the VPNP [19] or PIPE 4.3 [20] ToolKits. After obtaining parametric steady state probabilities $\pi_{i,k}$, they have to be converted to their corresponding fuzzy form $\tilde{\pi}_{i,k}$. To determine the steady state distribution fuzzy probability $\tilde{\pi}_{i,k}$ of this CTMC must solve this FFLSE by applying fuzzified transition firing rates**.** The matrix form of this FFLSE is $\tilde{\mathbf{A}} \otimes \tilde{\mathbf{x}} = \tilde{\mathbf{b}}$, where $\tilde{\mathbf{A}} = (\tilde{\mathbf{a}}_{i,j}) = (\tilde{a}_{i,j}, \tilde{\delta}_{i,j}, \tilde{\beta}_{i,j})$ is a $n \times n$ fuzzy matrix in which each element of $\tilde{\mathbf{A}}$ is a fuzzy number, and $\tilde{\mathbf{x}} = (\tilde{x}_1, \ldots, \tilde{x}_n)$, $\tilde{\mathbf{b}} = (\tilde{b}_1, \ldots, \tilde{b}_n)$ are fuzzy vectors $n \times 1$. We may represent fuzzy matrix $\tilde{\mathbf{A}} = (\tilde{\mathbf{a}}_{i,j})_{n \times n}$ with new notation $\tilde{\mathbf{A}} = (\mathbf{A}, \mathbf{M}, \mathbf{N})$, where $\mathbf{A} = (a_{i,j})$, $\mathbf{M} = (\delta_{i,j})$, and $\mathbf{M} = (\beta_{i,j})$ are three $n \times n$ crips matrices [21, 22]. Using the algebra multiplication of two fuzzy numbers on the $\tilde{\mathbf{A}} \otimes \tilde{\mathbf{x}} = \tilde{\mathbf{b}}$, where $\tilde{\mathbf{A}} = (\mathbf{A}, \mathbf{M}, \mathbf{N})$, $\tilde{\mathbf{x}} = (\mathbf{x}, \mathbf{y}, \mathbf{z})$ and $\tilde{\mathbf{b}} = (\mathbf{b}, \mathbf{g}, \mathbf{d})$, we obtain the formula $(\mathbf{A} \cdot \mathbf{x},\ \mathbf{A} \cdot \mathbf{y} + \mathbf{M} \cdot \mathbf{x},\ \mathbf{A} \cdot \mathbf{z} + \mathbf{N} \cdot \mathbf{x}) = (\mathbf{b}, \mathbf{g}, \mathbf{d})$, whereby the solution $\tilde{\mathbf{x}} = (\mathbf{x}, \mathbf{y}, \mathbf{z})$ is determined by solving the following three systems of equations in crips numbers [21, 22]:

$$\mathbf{A} \cdot \mathbf{x} = \mathbf{b};\ \mathbf{A} \cdot \mathbf{y} = \mathbf{g} - \mathbf{M} \cdot \mathbf{x};\ \mathbf{A} \cdot \mathbf{z} = \mathbf{d} - \mathbf{N} \cdot \mathbf{x}. \quad (1)$$

Let $M_{i,k}[u_{i,l} >$ is the continuous transition $u_{i,l}$ enabled by the current marking $M_{i,k}$ of the discrete part of the analyzed model $FSHPN$ [8, 9]. In this case the average aggregate data processing fuzzy speed $\overline{v}^{(i)}$ of Sv_i is determined by following expressons:

$$\overline{v}^{(i)} = \Big(\sum_{\forall M_{i,k}[u_{i,j}>} (\tilde{v}_{i,l}(M_{i,k}) \cdot \tilde{\pi}_{i,k}) \Big) / \sum_{\forall M_{i,k}[u_{i,j}>} \tilde{\pi}_{i,k},\ i = \overline{1, N}. \quad (2)$$

Also, let $M_{i,k}[t_{i,j} >$ it is the timed discrete transition $t_{i,j}$ enabled by the current marking $M_{i,k}$.

The average aggregate fuzzy rate $\overline{\lambda}^{(i)}$ of transition Sv_i *from active to passive state* is:

$$\overline{\lambda}^{(i)} = \Big(\sum_{\substack{\forall (M_{i,k}[t_{i,j}>) \wedge \\ (M_{i,k}[u_{i,l}>)}} \tilde{\lambda}_{i,j}(M_{i,k}) \cdot \tilde{\pi}_{i,k} \Big) / \Big(\sum_{\substack{\forall (M_{i,k}[t_{i,j}>) \wedge \\ (M_{i,k}[u_{i,l}>)}} \tilde{\pi}_{i,k} \Big),\ i = \overline{1, N}. \quad (3)$$

Also, the aggregate average fuzzy rate $\overline{\mu}^{(i)}$ of transition Sv_i from passive to active state is:

$$\overline{\mu}^{(i)} = \Big(\sum_{\forall (M_{i,n}[t_{i,m}>} \tilde{\mu}_{i,m}(M_{i,n}) \cdot \tilde{\pi}_{i,n} \Big) / \Big(\sum_{M_{i,k}[t_{i,j}>) \wedge} \tilde{\pi}_{i,n} \Big),\ i = \overline{1, N}. \quad (4)$$

Thus, determining the fuzzy parameters calculated according to the expressions (1) ... (3), we identify the respective fuzzy parameters of the aggregate model $SHPN2_i$ that describes the dipole DP_i behavior shown in Figure 8:

$$\overline{v}_1^{(i)} = \overline{v}^{(i)},\ \overline{v}_2^{(i)} = \overline{v}^{(i+1)},\ \overline{\lambda}_1^{(i)} = \overline{\lambda}^{(i)},\ \overline{\lambda}_2^{(i)} = \overline{\lambda}^{(i+1)},\ \overline{\mu}_1^{(i)} = \overline{\mu}^{(i)} \text{ și } \overline{\mu}_2^{(i)} = \overline{\mu}^{(i+1)}.$$

Based on these parameters, we can build the aggregate hybrid *FCMTC* to realize the performance evaluation of a dipole DP_i, and then they are used to evaluate the performance mesures of the entire analyzed *FSHPN* model. For this, în section 5 we present an algorithm in a fixed point iteration scheme for the analysis of a this type *FSHPN models*.

4. Aggregate HCTMC and performance analysis of a dipole

4.1. Aggregate HCTMC of a dipole

The aim of this section is to derive the formulas of the most important steady state performance measures of a dipole DP_i.

The behavior of SA_i and SD_i with two respectively aggregate states (*active* s_1 or passive s_2 state) of a dipole DP_i, $i=1,2,\cdots,N-1$ of the model $FSHPN\ 2_i$ is described by the aggregate fuzzy hybrid CTMC ($HCTMC\ 2_i$). The states of $HCTMC\ 2_i$ are described by the 4-tuple $(s_1, s_2, x_i; \overline{V}_k^{(i)})$, where $s_1,\ s_2 \in \{0,1\}, k=\overline{0,3}$, and $\overline{V}_k^{(i)} = s_1 \cdot \overline{v}_1^{(i)} - s_2 \cdot \overline{v}_2^{(i)}$ is the *dynamic balance* [??] that determine the speed of changing the fluid stock level x_i, $0 \le x_i \le h_i$, in the buffer b_i.

The state transition diagram of this $HCTMC\ 2_i$ depends on the concrete relationships between the values of $\overline{v}_1^{(i)}$ and $\overline{v}_2^{(i)}$, which can be: $\overline{v}_1^{(i)} = \overline{v}_2^{(i)}$, $\overline{v}_1^{(i)} > \overline{v}_2^{(i)}$ or $\overline{v}_1^{(i)} < \overline{v}_2^{(i)}$. The method of constructing these types of transition diagrams and writing on their basis the *Chapman-Kolmogorov equilibrium equations* is described in [9]. Figure 9a shows the transition diagram of $HCTMC\ 2_i$ for the internal states ($0 < x_i < h_i$) with *low* ($x_i = 0$) and *high* ($x_i = h_i$) boundary states for $\overline{v}_1^{(i)} < \overline{v}_2^{(i)}$, and in Figure 9b the one is presented for $\overline{v}_1^{(i)} > \overline{v}_2^{(i)}$.

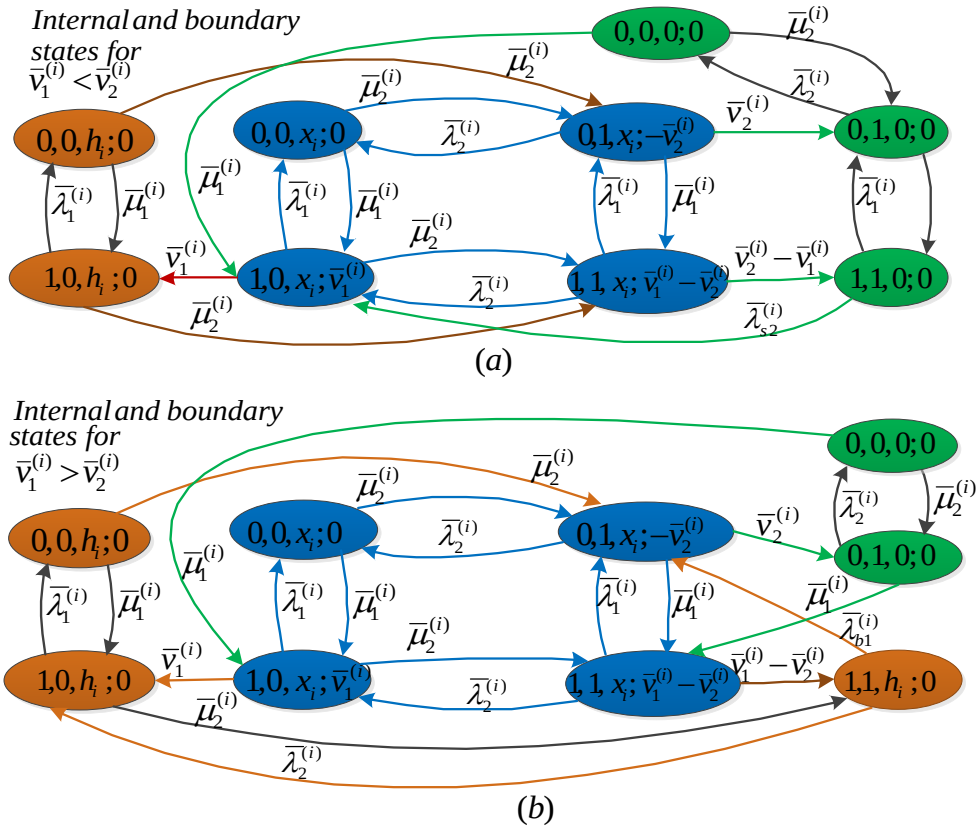

Figure 9. State transition diagrams of $HCTMC\ 2_i$ which describes the behaviour of $FSHPN\ 2_i$: (a) internal and boundary states with $\overline{v}_1^{(i)} < \overline{v}_2^{(i)}$; (b) internal and boundary states with $\overline{v}_1^{(i)} > \overline{v}_2^{(i)}$.

4.2. Aggregate HCTMC equations describing the evolution of a dipole

As, all the proposed models are bounded and the initial marking is a home state, the underlying $HCTMC\ 2_i$ of a dipole DP_i are ergodic for the different behavior fuzzy parameters.

The steady state density probability equations in the internal states of $HCTMC\ 2_i$. When the buffer b_i is neither empty nor full, the stock level x_i, $0 < x_i < h_i$, of this buffer varies with density probability $f_{s1,s2}^{(i)}(x_i)$ depending on the current internal state of the buffer b_i and adjacent servers. Because the level of the stock in b_i can vary very little over a short period of time, the behavior of the dipole DP_i in steady state regime for internal states is described by the following system of ordinary differential equations [7]:

$$0 = -(\overline{\mu}_1^{(i)} + \overline{\mu}_2^{(i)})\, f_{0,0}^{(i)}(x_i) + \overline{\lambda}_2^{(i)}\, f_{0,1}^{(i)}(x_i) + \overline{\lambda}_1^{(i)}\, f_{1,0}^{(i)}(x_i),$$

$$-\overline{v}_2^{(i)} \frac{\partial f_{0,1}^{(i)}(x_i)}{\partial x_i} = -(\overline{\mu}_1^{(i)} + \overline{\lambda}_2^{(i)})\, f_{0,1}^{(i)}(x_i) + \overline{\lambda}_1^{(i)}\, f_{1,1}^{(i)}(x_i) + \overline{\mu}_2^{(i)}\, f_{0,0}^{(i)}(x_i), \tag{5}$$

$$\overline{v}_1^{(i)} \frac{\partial f_{1,0}^{(i)}(x_i)}{\partial x_i} = -(\overline{\lambda}_1^{(i)} + \overline{\mu}_2^{(i)})\, f_{1,0}^{(i)}(x_i) + \overline{\lambda}_2^{(i)}\, f_{1,1}^{(i)}(x_i) + \overline{\mu}_1^{(i)}\, f_{0,0}^{(i)}(x_i),$$

$$(\overline{v}_1^{(i)} - \overline{v}_2^{(i)}) \frac{\partial f_{1,1}^{(i)}(x_i)}{\partial x_i} = -(\overline{\lambda}_1^{(i)} + \overline{\lambda}_2^{(i)})\, f_{1,1}^{(i)}(x_i) + \overline{\mu}_1^{(i)}\, f_{0,1}^{(i)}(x_i) + \overline{\mu}_2^{(i)}\, f_{1,0}^{(i)}(x). \tag{6}$$

The steady-state fuzzy probabilitie equations in the boundary states of $HCTMC\ 2_i$. While the internal behavior of the dipole DP_i can be described by probability densities, it can reach a certain boundary state with a fuzzy probability $\rho_{s1,s2}^{(i)}(0)$ or $\rho_{s1,s2}^{(i)}(h_i)$ different from zero. For example, if $\overline{v}_1^{(i)} > \overline{v}_2^{(i)}$ (resp. $\overline{v}_1^{(i)} < \overline{v}_2^{(i)}$) and both servers are operational, the stock x_i of buffer b_i tends to *increase* (resp. *to decrease*). If this situation lasts long enough, the buffer b_i will be *full* (resp. *empty*), we have $x_i = h_i$ (resp. $x_i = 0$) and the *dynamic balance* of stock in buffer b_i is $(\overline{v}_1^{(i)} - \overline{v}_2^{(i)}) = 0$. In this case it will reach the state $x_i = h_i$ and it will remain there until one of the two servers Sv_i or Sv_{i+1} it will not go into passive state.

From the transition diagrams presented in Figures 6 and Figures 7 respectively, for the *lower boundary*, $x_i = 0$, according to the method of writing the equilibrium equations of the steady-state probabilities described in [9], we obtain:

- for $\overline{v}_1^{(i)} > \overline{v}_2^{(i)}$ we have:

$$\text{if } x_i \to 0: (\overline{\mu}_1^{(i)} + \overline{\lambda}_2^{(i)}) \cdot \rho_{0,1}^{(i)}(0) = \overline{\mu}_2^{(i)} \cdot \rho_{0,1}^{(i)}(0) + \overline{v}_2^{(i)} \cdot f_{0,1}^{(i)}(0), \tag{7}$$

$$(\overline{\mu}_1^{(i)} + \overline{\mu}_2^{(i)}) \cdot \rho_{0,0}^{(i)}(0) = \overline{\lambda}_2^{(i)} \cdot \rho_{0,1}^{(i)}(0),$$

  - if $0 \to x_i$: $\quad \overline{v}_2^{(i)} \cdot f_{1,0}^{(i)}(0) = \overline{\mu}_1^{(i)} \cdot \rho_{0,0}^{(i)}(0)$, $\quad (\overline{v}_1^{(i)} - \overline{v}_2^{(i)})\, f_{1,1}^{(i)}(0) = \overline{\mu}_1^{(i)} \rho_{0,1}^{(i)}(0)$;

- for $\overline{v}_1^{(i)} < \overline{v}_2^{(i)}$ we have:

  - if $x_i \to 0$: $\quad (\overline{\mu}_1^{(i)} + \overline{\lambda}_2^{(i)}) \cdot \rho_{0,1}^{(i)}(0) = \overline{\mu}_2^{(i)} \cdot \rho_{0,0}^{(i)}(0) + \overline{\lambda}_1^{(i)} \cdot \rho_{1,1}^{(i)}(0) + \overline{v}_2^{(i)} \cdot f_{0,1}^{(i)}(0)$,

$$(\overline{\mu}_1^{(i)} + \overline{\mu}_2^{(i)}) \cdot \rho_{0,0}^{(i)}(0) = \overline{\lambda}_2^{(i)} \cdot \rho_{0,1}^{(i)}(0), \tag{8}$$

$$(\overline{\lambda}_1^{(i)} + \overline{\lambda}_{s2}^{(i)}) \cdot \rho_{1,1}^{(i)}(0) = \overline{\mu}_1^{(i)} \cdot \rho_{0,1}^{(i)}(0) + (\overline{v}_2^{(i)} - \overline{v}_1^{(i)}) \cdot f_{1,1}^{(i)}(0),$$

if $0 \to x_i$: $\overline{v}_1^{(i)} \cdot f_{1,0}^{(i)}(0) = \overline{\mu}_1^{(i)} \cdot \rho_{0,0}^{(i)}(0) + \overline{\lambda}_{s2}^{(i)} \cdot \rho_{1,1}^{(i)}(0)$, where: $\overline{\lambda}_{s2}^{(i)} = \overline{\lambda}_2^{(i)} \cdot \overline{v}_1^{(i)} / \overline{v}_2^{(i)}$.

Similarly, for the *upper boundary*, $x_i = h_i$, we obtain the following steady-state equations:

- for $\overline{v}_1^{(i)} > \overline{v}_2^{(i)}$ we have:
  - if $x_i \to h_i$: $(\overline{\lambda}_1^{(i)} + \overline{\mu}_2^{(i)}) \cdot \rho_{1,0}^{(i)}(h_i) = \overline{\lambda}_2^{(i)} \cdot \rho_{1,1}^{(i)}(h_i) + \overline{\mu}_1^{(i)} \cdot \rho_{0,0}^{(i)}(h_i) + \overline{v}_1^{(i)} \cdot f_{0,1}^{(i)}(h_i)$,

$$(\overline{\lambda}_{b1}^{(i)} + \overline{\lambda}_2^{(i)}) \cdot \rho_{1,1}^{(i)}(h_i) = \overline{\mu}_2^{(i)} \cdot \rho_{1,0}^{(i)}(h_i) + (\overline{v}_1^{(i)} - \overline{v}_2^{(i)}) \cdot f_{1,1}^{(i)}(h_i), \tag{9}$$

$$(\overline{\mu}_1^{(i)} + \overline{\mu}_2^{(i)}) \cdot \rho_{0,0}^{(i)}(h_i) = \overline{\lambda}_1^{(i)} \cdot \rho_{1,0}^{(i)}(h_i),$$

  - if $h_i \to x_i$: $\overline{v}_2^{(i)} \cdot f_{0,1}^{(i)}(h_i) = \overline{\lambda}_{b1}^{(i)} \cdot \rho_{1,1}^{(i)}(h_i) + \overline{\mu}_2^{(i)} \cdot \rho_{0,0}^{(i)}(h_i)$, where: $\overline{\lambda}_{b1}^{(i)} = \overline{\lambda}_2^{(i)} \cdot \overline{v}_1^{(i)} / \overline{v}_2^{(i)}$;
- for $\overline{v}_1^{(i)} < \overline{v}_2^{(i)}$ we have:
  - if $x_i \to h_i$: $(\overline{\lambda}_1^{(i)} + \overline{\mu}_2^{(i)}) \cdot \rho_{1,0}^{(i)}(h_i) = \overline{\mu}_1^{(i)} \cdot \rho_{0,0}^{(i)}(h_i) + \overline{v}_1^{(i)} \cdot f_{1,0}^{(i)}(h_i)$,

$$(\overline{\mu}_1^{(i)} + \overline{\mu}_2^{(i)}) \cdot \rho_{0,0}^{(i)}(h_i) = \overline{\lambda}_1^{(i)} \cdot \rho_{0,1}^{(i)}(h_i), \tag{10}$$

  - if $h_i \to x_i$: $(\overline{v}_2^{(i)} - \overline{v}_1^{(i)}) \cdot f_{1,1}^{(i)}(h_i) = \overline{\mu}_2^{(i)} \cdot \rho_{1,0}^{(i)}(h_i)$, $\overline{v}_2^{(i)} \cdot f_{0,1}^{(i)}(h_i) = \overline{\mu}_2^{(i)} \cdot \rho_{0,0}^{(i)}(h_i)$.

The normalization equation. Since the sum of all probabilities must be equal to 1, we have:

$$\sum_{s_1=0,1} \sum_{s_2=0,1} [\int_0^{h_i} f_{s_1,s_2}^{(i)}(x_i) dx_i + \rho_{s_1,s_2}^{(i)}(0) + \rho_{s_1,s_2}^{(i)}(h_i)] = 1. \tag{11}$$

Performance measures of the system:

- *The average level* $\overline{x}_i$ *of stock in buffer* b_i. This QoS indicator is determined can be determined from the following expression:

$$\overline{x}_i = \sum_{s_1=0,1} \sum_{s_2=0,1} [\int_0^{h_i} x_i \cdot f_{s_1,s_2}^{(i)}(x_i) dx_i + h_i \cdot \rho_{s_1,s_2}^{(i)}(h_i)]. \tag{12}$$

- *The average data processing productivity* (*throughput*) $\overline{\eta}_{v2}^{(i)}$ by DP_i represents the *average speed* at which the fluid leaves the downstream server $SD_i = Sv_{i+1}$ of the buffer b_i. When the stock is not empty and SD_i it is operational, its speed is $\overline{v}_2^{(i)}$, and when the stock is empty and both servers SA_i and SD_i are operational, then its processing speed is equal to $\overline{v}_1^{(i)}$, so the $\overline{\eta}_{v2}^{(i)}$ is:

$$\overline{\eta}_{v2}^{(i)} = \overline{v}_2^{(i)} [\int_0^{h_i} (f_{0,1}^{(i)}(x_i) + f_{1,1}^{(i)}(x_i)) dx_i + \rho_{1,1}^{(i)}(h_i)] + \min(\overline{v}_1^{(i)}, \overline{v}_2^{(i)}) \cdot \rho_{1,1}^{(i)}(0). \tag{13}$$

Similarly, we calculate the throughput $\overline{\eta}_1^{(i)}$ of DP_i, which represents the average speed at which the fluid enters the buffer b_i.

We mention that the conservation of the flux in the dipole DP_i considered for $\overline{\eta}_{v1}^{(i)} = \overline{\eta}_{v2}^{(i)}$, $0 \le x_i \le h_i$, is given by the following equation:

$$(\overline{v}_2^{(i)} - \overline{v}_1^{(i)}) f_{1,1}(x_i) + \overline{v}_2^{(i)} f_{0,1}(x_i) - \overline{v}_1^{(i)} f_{1,0}(x_i) = 0. \quad (14)$$

4. 3. Performances evaluation of a dipole

In order to evaluate the performances measures of a dipole DP_i, it is necessary to considers and analyze separately the following three cases: $\overline{v}_1^{(i)} = \overline{v}_2^{(i)} = \overline{v}^{(i)}$, $\overline{v}_1^{(i)} > \overline{v}_2^{(i)}$ and $\overline{v}_1^{(i)} < \overline{v}_2^{(i)}$.

Due to the space restriction we will further analyze only the $\overline{v}_1^{(i)} \neq \overline{v}_2^{(i)}$**.** For $\overline{v}_1^{(i)} \neq \overline{v}_2^{(i)}$ from equations (12) and (13) the analytical solutions of system equations (12) and (12), which describe the evolution of $HCTMC\ 2_i$, taking into account the boundary equations (12) for two separate cases: $\overline{v}_1^{(i)} > \overline{v}_2^{(i)}$ and $\overline{v}_1^{(i)} < \overline{v}_2^{(i)}$, are determined by the following expressions:

- internal states, $0 < x_i < h_i$:

$$f_{1,0}^{(i)}(x_i) = C_0^{(i)} \cdot A_1^{(i)} \cdot e^{r^{(i)} \cdot x_i}, \quad f_{0,1}^{(i)}(x_i) = C_0^{(i)} \cdot e^{r^{(i)} \cdot x_i}, \quad (15)$$

$$f_{0,0}^{(i)}(x_i) = C_0^{(i)} \cdot A_2^{(i)} \cdot e^{r^{(i)} \cdot x_i}, \quad f_{1,1}^{(i)}(x_i) = C_0^{(i)} \cdot A_3^{(i)} \cdot e^{r^{(i)} \cdot x_i};$$

- boundary states for $x_i = 0$: $\rho_{1,0}^{(i)}(0) = 0,$

$$\rho_{0,0}^{(i)}(0) = \begin{cases} C_0^{(i)} \cdot \overline{v}_1^{(i)} \cdot A_1^{(i)} / \overline{\mu}_1^{(i)} & if \ \ \overline{v}_1^{(i)} > v_2^{(i)} \\ C_0^{(i)} \cdot \overline{\lambda}_2^{(i)} \cdot C_2^{(i)} / ((\overline{\mu}_1^{(i)} + \overline{\mu}_2^{(i)}) \cdot A_4^{(i)}) & if \ \overline{v}_1^{(i)} < \overline{v}_2^{(i)} \end{cases}, \quad (16)$$

$$\rho_{0,1}^{(i)}(0) = \begin{cases} C_0^{(i)} \cdot \overline{v}_1^{(i)} \cdot A_1^{(i)} \cdot (\overline{\mu}_1^{(i)} + \overline{\mu}_2^{(i)}) / (\overline{\lambda}_2^{(i)} \cdot \overline{\mu}_1^{(i)}) & if \ \ \overline{v}_1^{(i)} > v_2^{(i)} \\ C_0^{(i)} \cdot C_2^{(i)} / A_4^{(i)} & if \ \overline{v}_1^{(i)} < \overline{v}_2^{(i)} \end{cases},$$

$$\rho_{1,1}^{(i)}(0) = \begin{cases} 0 & if \ \overline{v}_1^{(i)} > v_2^{(i)} \\ C_0^{(i)} \cdot C_1^{(i)} / A_4^{(i)} & if \ \overline{v}_1^{(i)} < \overline{v}_2^{(i)} \end{cases};$$

- boundary states for $x_i = h_i$: $\rho_{0,1}^{(i)}(h_i) = 0,$

$$\rho_{0,0}^{(i)}(h_i) = \begin{cases} C_0^{(i)} \cdot C_2^{(i)} \cdot \overline{\lambda}_1^{(i)} / ((\overline{\mu}_1^{(i)} + \overline{\mu}_2^{(i)}) \cdot A_4^{(i)}) & if \ \ \overline{v}_1^{(i)} > v_2^{(i)} \\ C_0^{(i)} \cdot \overline{v}_2^{(i)} \cdot e^{r^{(i)} \cdot x_i} / \overline{\mu}_2^{(i)} & if \ \ \overline{v}_1^{(i)} < \overline{v}_2^{(i)} \end{cases},$$

$$\rho_{1,0}^{(i)}(h_i) = \begin{cases} C_0^{(i)} \cdot C_2^{(i)} / A_4^{(i)} & if \ \ \overline{v}_1^{(i)} > v_2^{(i)} \\ C_0^{(i)} \cdot (\overline{v}_2^{(i)} - \overline{v}_1^{(i)}) \cdot A_3^{(i)} \cdot e^{r^{(i)} \cdot x_i} / \overline{\mu}_2^{(i)} & if \ \ \overline{v}_1^{(i)} < \overline{v}_2^{(i)} \end{cases}, \quad (17)$$

$$\rho_{1,1}^{(i)}(h_i) = \begin{cases} C_0^{(i)} \cdot C_1^{(i)} / A_4^{(i)} & if \ \ \overline{v}_1^{(i)} > v_2^{(i)} \\ 0 & if \ \ \overline{v}_1^{(i)} < \overline{v}_2^{(i)} \end{cases},$$

where:
$$r^{(i)}=\begin{cases}(E_1^{(i)}\cdot E_4^{(i)}-E_2^{(i)}\cdot E_3^{(i)})/(E_1^{(i)}-E_3^{(i)}) & if\ \ \bar{v}_1^{(i)}>v_2^{(i)}\\ (E_1^{(i)}\cdot E_4^{(i)}-E_2^{(i)}\cdot E_3^{(i)})/(E_3^{(i)}-E_1^{(i)}) & if\ \ \bar{v}_1^{(i)}<\bar{v}_2^{(i)}\end{cases}$$

$$A_2^{(i)}=[\bar{\lambda}_2^{(i)}\cdot(E_1^{(i)}-E_3^{(i)})+\bar{\lambda}_1^{(i)}\cdot(E_4^{(i)}-E_2^{(i)})]/[(E_1^{(i)}-E_3^{(i)})\cdot(\bar{\mu}_1^{(i)}+\bar{\mu}_2^{(i)})],$$

$$A_3^{(i)}=[\bar{v}_2^{(i)}\cdot(E_1^{(i)}-E_3^{(i)})+\bar{v}_1^{(i)}\cdot(E_4^{(i)}-E_2^{(i)})]/[(E_1^{(i)}-E_3^{(i)})\cdot(\bar{v}_1^{(i)}-\bar{v}_2^{(i)})],$$

$$E_1^{(i)}=(\bar{\lambda}_2^{(i)}\cdot\omega_1^{(i)}-\bar{\mu}_2^{(i)}\cdot\omega_2^{(i)})/\bar{v}_1^{(i)}\ ,\ \ E_2^{(i)}=-\bar{\lambda}_2^{(i)}\cdot\omega_1^{(i)}/\bar{v}_1^{(i)}\ ,\ \ E_3^{(i)}=-\bar{\lambda}_1^{(i)}\cdot\omega_1^{(i)}/\bar{v}_2^{(i)}$$

$$E_4^{(i)}=(\bar{\lambda}_1^{(i)}\cdot\omega_1^{(i)}+\bar{\mu}_1^{(i)}\cdot\omega_2^{(i)})/\bar{v}_2^{(i)},\ A_1^{(i)}=(E_2^{(i)}-E_4^{(i)})/(E_3^{(i)}-E_1^{(i)}),$$

$$\omega_1^{(i)}=(\bar{v}_1^{(i)}\cdot\bar{\mu}_1^{(i)}+\bar{v}_2^{(i)}\cdot\bar{\mu}_2^{(i)})/((\bar{v}_2^{(i)}-\bar{v}_1^{(i)})(\bar{\mu}_1^{(i)}+\bar{\mu}_2^{(i)}))\,,\ \omega_2^{(i)}=1+(\bar{\lambda}_1^{(i)}+\bar{\lambda}_2^{(i)})/(\bar{\mu}_1^{(i)}+\bar{\mu}_2^{(i)})\,,$$

$$A_4^{(i)}=\begin{cases}\bar{\lambda}_1^{(i)}\cdot(\bar{\lambda}_2^{(i)}+(\bar{\lambda}_1^{(i)}+\bar{\mu}_1^{(i)}+\bar{\mu}_2^{(i)})\cdot\bar{v}_2^{(i)}/\bar{v}_1^{(i)}) & if\ \ \bar{v}_1^{(i)}>v_2^{(i)}\\ \bar{\lambda}_2^{(i)}\cdot(\bar{\lambda}_1^{(i)}+(\bar{\lambda}_2^{(i)}+\bar{\mu}_1^{(i)}+\bar{\mu}_2^{(i)})\cdot\bar{v}_1^{(i)}/\bar{v}_2^{(i)}) & if\ \ \bar{v}_1^{(i)}<\bar{v}_2^{(i)}\end{cases}$$

$$C_1^{(i)}=\begin{cases}[\bar{v}_1^{(i)}\cdot(\bar{\mu}_1^{(i)}+\bar{\mu}_2^{(i)})+(\bar{\lambda}_1^{(i)}+\bar{\mu}_1^{(i)}+\bar{\mu}_2^{(i)})\cdot(\bar{v}_1^{(i)}-\bar{v}_2^{(i)})\cdot A_3^{(i)}]\cdot e^{r^{(i)}\cdot h_i} & if\ \ \bar{v}_1^{(i)}>v_2^{(i)}\\ \bar{v}_2^{(i)}\cdot(\bar{\mu}_1^{(i)}+\bar{\mu}_2^{(i)})+(\bar{\lambda}_2^{(i)}+\bar{\mu}_1^{(i)}+\bar{\mu}_2^{(i)})\cdot(\bar{v}_2^{(i)}-\bar{v}_1^{(i)})\cdot A_3^{(i)} & if\ \ \bar{v}_1^{(i)}<\bar{v}_2^{(i)}\end{cases}$$

$$C_2^{(i)}=\begin{cases}(\bar{\mu}_1^{(i)}+\bar{\mu}_2^{(i)})\cdot[\bar{\lambda}_1^{(i)}\cdot\bar{v}_2^{(i)}+\bar{\lambda}_2^{(i)}\cdot\bar{v}_1^{(i)}+\bar{\lambda}_2^{(i)}\cdot(\bar{v}_1^{(i)}-\bar{v}_2^{(i)})\cdot A_3^{(i)}]\cdot e^{r^{(i)}\cdot h_i}/\bar{\mu}_2^{(i)} & if\ \ \bar{v}_1^{(i)}>v_2^{(i)}\\ (\bar{\mu}_1^{(i)}+\bar{\mu}_2^{(i)})\cdot[\bar{\lambda}_1^{(i)}\cdot\bar{v}_2^{(i)}+\bar{\lambda}_2^{(i)}\cdot\bar{v}_1^{(i)}+\bar{\lambda}_1^{(i)}\cdot(\bar{v}_2^{(i)}-\bar{v}_1^{(i)})\cdot A_3^{(i)}]/\bar{\mu}_1^{(i)} & if\ \ \bar{v}_1^{(i)}<\bar{v}_2^{(i)}\end{cases}$$

$$D_1^{(i)}=(1+A_1^{(i)}+A_2^{(i)}+A_3^{(i)})\cdot(e^{r^{(i)}\cdot h_i}-1)/r^{(i)},\quad D_2^{(i)}=\bar{v}_1^{(i)}\cdot A_1^{(i)}\cdot(1+(\bar{\mu}_1^{(i)}+\bar{\mu}_2^{(i)})/\bar{\lambda}_2^{(i)}),$$

$$D_3^{(i)}=C_1^{(i)}+C_2^{(i)}\cdot(1+\bar{\lambda}_1^{(i)}/(\bar{\mu}_1^{(i)}+\bar{\mu}_2^{(i)})),$$

$$A_4^{(i)}=\begin{cases}\bar{\lambda}_1^{(i)}\cdot(\bar{\lambda}_2^{(i)}+(\bar{\lambda}_1^{(i)}+\bar{\mu}_1^{(i)}+\bar{\mu}_2^{(i)})\cdot\bar{v}_2^{(i)}/\bar{v}_1^{(i)}) & if\ \ \bar{v}_1^{(i)}>v_2^{(i)}\\ \bar{\lambda}_2^{(i)}\cdot(\bar{\lambda}_1^{(i)}+(\bar{\lambda}_2^{(i)}+\bar{\mu}_1^{(i)}+\bar{\mu}_2^{(i)})\cdot\bar{v}_1^{(i)}/\bar{v}_2^{(i)}) & if\ \ \bar{v}_1^{(i)}<\bar{v}_2^{(i)}\end{cases}$$

$$D_4^{(i)}=(1+A_1^{(i)}+A_2^{(i)}+A_3^{(i)})\cdot[(r^{(i)}\cdot h_i-1)\cdot e^{r^{(i)}\cdot h_i}+1]/(r^{(i)})^2,$$

$$G_3^{(i)}=[C_1^{(i)}+C_2^{(i)}\cdot(1+\bar{\lambda}_2^{(i)}/(\bar{\mu}_1^{(i)}+\bar{\mu}_2^{(i)}))]/A_4^{(i)},\ \ G_4^{(i)}=[\bar{v}_2^{(i)}\cdot A_2^{(i)}+(\bar{v}_2^{(i)}-\bar{v}_1^{(i)})\cdot A_3^{(i)}]\cdot e^{r^{(i)}\cdot h_i}/\bar{\mu}_2^{(i)},$$

$$C_0^{(i)}=\begin{cases}1/(D_1^{(i)}+D_2^{(i)}+D_3^{(i)}) & if\ \ \bar{v}_1^{(i)}>\bar{v}_2^{(i)}\\ 1/(D_1^{(i)}+G_3^{(i)}+G_4^{(i)}) & if\ \ \bar{v}_1^{(i)}<\bar{v}_2^{(i)}\end{cases}.$$

For $r^{(i)}\neq 0$ and $\bar{v}_1^{(i)}\neq\bar{v}_2^{(i)}$ based on the above expressions we determine the following performance measures of isolated DP_i:

- The *average throughput* $\bar{\eta}_{v2}^{(i)}$ of data processing is:

$$\bar{\eta}_{v2}^{(i)}=\begin{cases}C_0^{(i)}\cdot\bar{v}_2^{(i)}\cdot(1+A_3^{(i)})\cdot(e^{r^{(i)}\cdot h_i}-1)/r^{(i)}) & if\ \ \bar{v}_1^{(i)}>v_2^{(i)}\\ C_0^{(i)}\cdot[(\bar{v}_2^{(i)}\cdot(1+A_3^{(i)})\cdot(e^{r^{(i)}\cdot h_i}-1)/r^{(i)})+\bar{v}_1^{(i)}\cdot C_1^{(i)}/A_4^{(i)})] & if\ \ \bar{v}_1^{(i)}<\bar{v}_2^{(i)}\end{cases};\qquad(18)$$

- The *average level* $\bar{x}_i=[x_i^-,\,x_i^+]$ *of stock in buffer* b_i is given by the expression:

$$\bar{x}_i=\begin{cases}C_0^{(i)}\cdot(h_i\cdot D_3^{(i)}+D_4^{(i)}) & if\ \ \bar{v}_1^{(i)}>\bar{v}_2^{(i)}\\ C_0^{(i)}\cdot(h_i\cdot G_4^{(i)}+D_4^{(i)}) & if\ \ \bar{v}_1^{(i)}<\bar{v}_2^{(i)}\end{cases};\qquad(19)$$

- The Sv_{i+1} *starvation probability* $\rho_{ST_2}^{(i)} = [\rho_{ST_2}^{-(i)}, \rho_{ST_2}^{+(i)}]$ of dipole DP_i is:

$$\rho_{ST_2}^{(i)} = \sum_{s_1=0,\,1} \sum_{s_2=0,\,1} \rho_{s_1,s_2}^{(i)}(0);$$

- The Sv_i *blocking probability* $\rho_{BL_1}^{(i)} = [\rho_{BL_1}^{-(i)}, \rho_{BL_1}^{+(i)}]$ of dipole DP_i is:

$$\rho_{BL_1}^{(i)} = \sum_{s_1=0,\,1} \sum_{s_2=0,\,1} \rho_{s_1,s_2}^{(i)}(h_i);$$

- The Sv_{i+1} *average temporal redundancy* $\bar{\tau}_i = [\bar{\tau}_i^-, \bar{\tau}_i^+]$ of dipole DP_i is: $\bar{\tau}_i = \bar{x}_i / \bar{\eta}_{v2}^{(i)}$.

4.4. Numerical case study for performances analysis of a dipole

Next we will present a case study to show the use of the approach presented in this paper. The numerical analysis of some performance measures is based on the use of the $HCTMC\ 2_i$ model, using the knowledge of the experts in the field [10]. As example for the fuzzy rates $\tilde{\lambda}_j$ of discrete transitions and speeds $\tilde{v}_l$ of continuous transitions, we establish the following TNFs values: $\tilde{a} = (a, \delta, \beta)$, on the other hand, a parametric $\alpha - cut$ fuzzy number $\tilde{a} = [a^-(\alpha), a^+(\alpha)]$, $\tilde{a} \in \{\tilde{\lambda}_j, \tilde{v}_l\}$ can be represented as: $a^-(\alpha) = a - (1-\alpha)\delta$ and $a^+(\alpha) = a + (1-\alpha)\beta$.

The transition diagrams of the accessibility graph ($AcG1_i$) with symbolic marking [4, 5] and of the fuzzy Markov continuous time chain ($FCMTC1_i$), which describes the behavior of the discrete part of $FGSPN_{Svi}$ model in Figure 7, are shown respectively in Figure 10a and Figure 10b.

The steady state fully fuzzy linear system of Chapman-Kolmogorov equations, that describes the Markov process behavior $FCMTC1_i$ of discrete part $FGSPN_{Svi}$, is:

$$\tilde{\lambda}_{i,1}\cdot\tilde{\pi}_{i,0} - \tilde{\lambda}_{i,5}\cdot\tilde{\sigma}_{i,7}\cdot\tilde{\pi}_{i,2} - \tilde{\lambda}_{i,8}\cdot\tilde{\pi}_{i,3} = 0; \quad \tilde{\lambda}_{i,4}\cdot\tilde{\pi}_{i,1} - \tilde{\lambda}_{i,1}\cdot\tilde{\sigma}_{i,2}\cdot\tilde{\pi}_{i,0} = 0; \tag{20}$$

$$\tilde{\lambda}_{i,5}\cdot\tilde{\pi}_{i,2} - \tilde{\lambda}_{i,1}\cdot\tilde{\sigma}_{i,3}\cdot\tilde{\pi}_{i,0} - \tilde{\lambda}_{i,4}\cdot\tilde{\pi}_{i,1} = 0; \quad \tilde{\pi}_{i,0} + \tilde{\pi}_{i,1} + \tilde{\pi}_{i,2} + \tilde{\pi}_{i,3} = 1; \quad \tilde{\sigma}_{i,2} + \tilde{\sigma}_{i,3} = 1; \quad \tilde{\sigma}_{i,6} + \tilde{\sigma}_{i,7} = 1.$$

where: $0 < \tilde{\sigma}_{i,2} = \tilde{w}_{i,2}/(\tilde{w}_{i,2} + \tilde{w}_{i,3}) < 1,\ 0 < \tilde{\sigma}_{i,7} = \tilde{w}_{i,7}/(\tilde{w}_{i,6} + \tilde{w}_{i,7}) < 1.$

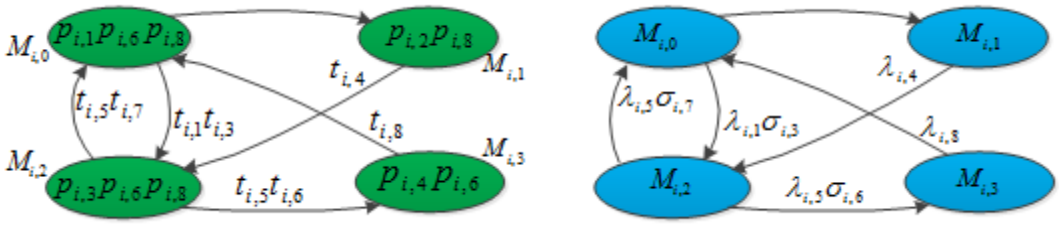

Figure 10. The states transition diagrams of the discrete part $FSHPN1_i$: a) $AcG1_i$; b) $FCMTC1_i$.

To illustrate this approach, we analyzed the $FSHPN1_i$ model of dipole DP_i with the follo-wing value of the fuzzy parameters for Sv_i and Sv_{i+1}:

$$\tilde{\lambda}_{i,1}=(0.3,0.1,0.1),\ \ \tilde{\lambda}_{i,4}=(0.8,0.3,0.2),\ \ \tilde{\lambda}_{i,5}=(0.5,0.3,0.1),\ \ \tilde{\lambda}_{i,8}=(0.9,0.2,0.2),\ \ \tilde{\sigma}_{i,2}=(0.8,0.0,0.0),$$
$$\tilde{\sigma}_{i,3}=(0.2,0.0,0.0),\ \ \tilde{\sigma}_{i,7}=(0.2,0.0,0.0),\ \tilde{v}_{i,1}=(5.0,2.0,3.0),\ \ \tilde{v}_{i,2}=(3.0,1.0,2.0);$$
$$\tilde{\lambda}_{i+1,1}=(0.2,0.1,0.3),\ \ \tilde{\lambda}_{i+1,4}=(0.6,0.2,0.2),\ \ \tilde{\lambda}_{i+1,5}=(0.6,0.2,0.3),\ \ \tilde{\lambda}_{i+1,8}=(0.8,0.3,0.2),\ \ \tilde{\sigma}_{i+1,2}=(0.7,0.0,0.0),$$
$$\tilde{\sigma}_{i+1,3}=(0.3,0.0,0.0),\ \ \tilde{\sigma}_{i+1,7}=(0.3,0.0,0.0),\ \tilde{v}_{i+1,1}=(4.0,2.0,1.0),\ \ \tilde{v}_{i+1,2}=(2.0,1.0,2.0).$$

For these fuzzy parameters, the solutions $\tilde{\pi}_{i,j}=[\tilde{\pi}^{-}_{i,j}(\alpha),\ \tilde{\pi}^{+}_{i,j}(\alpha)]$, $i=\overline{1,N-1}$ and $j=i+1$ of Chapman-Kolmogorov equation system (1) in $\alpha-cut$ parametric fuzzy numbers are obtained based on the methods presented in [10] and using respective MatLab Tool programs. These solutions, applicable to $0.34\le\alpha\le 1$, are the following:

$$\tilde{\pi}_{i,0}=[(0.461538463-(1-\alpha)\cdot 0.541001972),\ (0.461538463+(1-\alpha)\cdot 0.489067061)\ ],$$
$$\tilde{\pi}_{i,1}=[(0.138461538-(1-\alpha)\cdot 0.111531361),\ (0.138461538+(1-\alpha)\cdot 0.112681657)\ ],$$
$$\tilde{\pi}_{i,2}=[(0.276923076-(1-\alpha)\cdot 0.162139645),\ (0.276923076+(1-\alpha)\cdot 0.238055621)\ ],$$
$$\tilde{\pi}_{i,3}=[(0.123076923-(1-\alpha)\cdot 0.185327022),\ (0.123076923+(1-\alpha)\cdot 0.160195661)\ ];$$
$$\tilde{\pi}_{i+1,0}=[(0.574162671-(1-\alpha)\cdot 0.534709159),\ (0.574162671+(1-\alpha)\cdot 0.534709159)\ ],\quad(21)$$
$$\tilde{\pi}_{i+1,1}=[(0.133971292-(1-\alpha)\cdot 0.096212717),\ (0.133971292+(1-\alpha)\cdot 0.078611624)\ ],$$
$$\tilde{\pi}_{i+1,2}=[(0.191387568-(1-\alpha)\cdot 0.138088202),\ (0.191387568+(1-\alpha)\cdot 0.081045853)\ ],$$
$$\tilde{\pi}_{i+1,3}=[(0.100478469-(1-\alpha)\cdot 0.145546670),\ (0.100478469+(1-\alpha)\cdot 0.305633359)\ ];$$
$$\tilde{v}_{i,1}=[(5.0-(1-\alpha)\cdot 2.0),\ (5.0+(1-\alpha)\cdot 3.0)];\quad \tilde{v}_{i,2}=[(3.0-(1-\alpha)\cdot 1.0),\ (3.0+(1-\alpha)\cdot 2.0)],$$
$$\tilde{v}_{i+1,1}=[(4.0-(1-\alpha)\cdot 2.0),\ (4.0+(1-\alpha)\cdot 1.0)];\quad \tilde{v}_{i+1,2}=[(2.0-(1-\alpha)\cdot 1.0),\ (2.0+(1-\alpha)\cdot 2.0)].$$

Thus, using the relations (1), (2) and (3) the respective fuzzy parameters of the aggregate model $FSHPN2_i$ are calculated giving the following expressions:

$$\bar{v}_1^{(i)}=(\tilde{v}_{i,1}\tilde{\pi}_{i,0}+\tilde{v}_{i,2}\tilde{\pi}_{i,1})/(\tilde{\pi}_{i,0}+\tilde{\pi}_{i,1}),\quad \bar{v}_2^{(i)}=(\tilde{v}_{i+1,1}\tilde{\pi}_{i+1,0}+\tilde{v}_{i+1,2}\tilde{\pi}_{i+1,1})/(\tilde{\pi}_{i+1,0}+\tilde{\pi}_{i+1,1}),$$
$$\bar{\lambda}_1^{(i)}=(\tilde{\lambda}_{i,1}\tilde{\sigma}_{i,3}\tilde{\pi}_{i,0}+\tilde{\lambda}_{i,4}\tilde{\pi}_{i,1})/(\tilde{\pi}_{i,0}+\tilde{\pi}_{i,1}),\quad \bar{\lambda}_2^{(i)}=(\tilde{\lambda}_{i+1,1}\tilde{\sigma}_{i+1,3}\tilde{\pi}_{i+1,0}+\tilde{\lambda}_{i+1,4}\tilde{\pi}_{i,1})/(\tilde{\pi}_{i+1,0}+\tilde{\pi}_{i+1,1}),\quad(22)$$
$$\bar{\mu}_1^{(i)}=(\tilde{\lambda}_{i,5}\tilde{\sigma}_{i,7}\tilde{\pi}_{i,2}+\tilde{\lambda}_{i,8}\tilde{\pi}_{i,3})/(\tilde{\pi}_{i,2}+\tilde{\pi}_{i,3}),\quad \bar{\mu}_2^{(i)}=(\tilde{\lambda}_{i+1,5}\tilde{\sigma}_{i+1,7}\tilde{\pi}_{i+1,2}+\tilde{\lambda}_{i+1,8}\tilde{\pi}_{i+1,3})/(\tilde{\pi}_{i+1,2}+\tilde{\pi}_{i+1,3}).$$

Based on the expressions (22) the fuzzy parameters of the $FSHPN2_i$ model are:

$$\bar{v}_1^{(i)}=[(4.538487178-(1-\alpha)\cdot 3.512342402),\ (4.538487178+(1-\alpha)\cdot 2.626924617)];$$
$$\bar{v}_2^{(i)}=[(3.621621624-(1-\alpha)\cdot 0.237395463),\ (3.621621621+(1-\alpha)\cdot 3.160870372)];$$
$$\bar{\lambda}_1^{(i)}=[(0.259415519-(1-\alpha)\cdot 0.230759743),\ (0.230759743+(1-\alpha)\cdot 1.510542433)];\quad(23)$$
$$\bar{\lambda}_2^{(i)}=[(0.145945946-(1-\alpha)\cdot 0.133378811),\ (0.145945946+(1-\alpha)\cdot 0.123051021)];$$
$$\bar{\mu}_1^{(i)}=[(0.346153847-(1-\alpha)\cdot 0.063555446),\ (0.346153847+(1-\alpha)\cdot 0.063555446)].$$

Using these TFN values we can respectively determine the specified performance measures of the dipole DP_i. For instance, Figure 11 and Figure 12 show the effects of the $\alpha-cut$ and *buffer capacity* h_i on the *average throughput* $\bar{\eta}_{v2}^{+(i)}(\alpha,h_i)$, average level stock $\bar{x}_i^{-}(\alpha,h_i)$, starvation probability $\rho_{ST_2}^{+(i)}(\alpha,h_i)$ of Sv_{i+1} and the blocking probability $\rho_{BL_1}^{+(i)}(\alpha,h_i)$ of Sv_i.

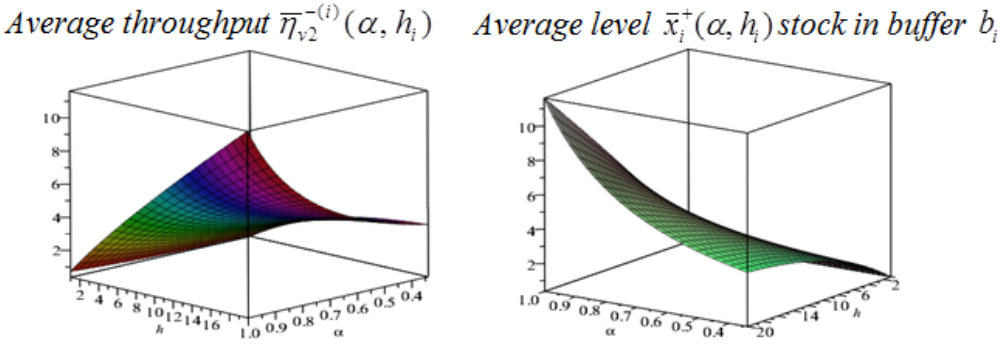

Figure 11. The average throughput $\overline{\eta}_{v2}^{+(i)}(\alpha, h_i)$ and the average level stock $\overline{x}_i^{-}(\alpha, h_i)$ in buffer b_i of dipole DP_i.

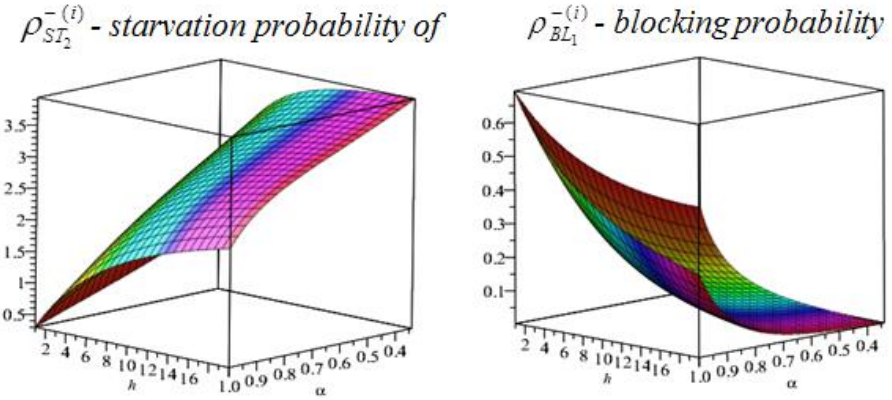

Figure 12. The starvation probability $\rho_{ST_2}^{+(i)}(\alpha, h_i)$ of Sv_{i+1} and the blocking probability $\rho_{BL_1}^{+(i)}(\alpha, h_i)$ of Sv_i.

5. Performance evaluation of buffer pipe-line *FSHPN* models

5.1. Update parameters of dipoles

Value evaluation of the DP_i aggregate parameters interaction dependents with the adjacent dipoles. In order to take into account the behaviour interdependence of the adjacent dipoles with DP_i it is necessary to include the *starvation states* of server SA_i and the *blocking states* of the server SD_i in their passive states [13, 14]. That is why it is necessary that the rates of change of states and the processing speed of the respective servers have to be adjusted. The rest of this subsection refers to the determination of the quantitative parameters of these aggregate passive states. Recall that SA_i of the considered dipole DP_i corresponds to the upstream server SD_{i-1} of the dipole DP_i, and SD_i corresponds to the downstream server SA_{i+1} of the dipole DP_i. First, we determine the aggregate average parameters for the server SA_i, after which the server SD_i parameters will be identified in a similar way. For this we use *upstream* and *downstream* dipole information, assuming we have all the necessary information. Then we get the aggregate rates of change of the respective states for SA_i by linking them together. So, for SA_i, the behavior aggregate state space contain three aggregate states: state where SA_i is *active* and producing fluid flow; *passiv* state where SA_i is not producing fluid flow because of a breakdown of the underlying server Sv_i (*down*), and state where SA_i is not producing fluid flow because it has no input (*starved*). These three aggregate states are formally defined as follows: 1) the SA_i is in *active state*

when Sv_i is *active*, and either buffer b_{i-1} is not empty and SA_{i-1} is *active*; 2) the SA_i is in *passive state* when Sv_i is *passive*; SA_i is starved when Sv_i is *active*, b_{i-1} is *empty*, and SA_{i-1} is in *passive state* or *starved*. For SA_i (resp. SD_i) of the dipole DP_i, we determine the aggregate rate $\overline{\lambda}_A^{(i)}$ (resp. $\overline{\lambda}_D^{(i)}$) transition from the active state to the passive state and the aggregate rate $\overline{\mu}_A^{(i)}$ (resp. $\overline{\mu}_D^{(i)}$) transition from the passive state to the active state. Also, we determine the average aggregate speed $\overline{v}_A^{(i)}$ (resp. $\overline{v}_D^{(i)}$) of data processing by the respective server in the active state, which is not necessarily equal to the specified maximum speed, because it may be the case that the server sometimes has to adjust its speed because of a slower upstream server and an empty buffer.In this case, we use the following information from the upstream dipole (or downstream dipole):

- $\overline{\pi}_{j,j'}^{(i-1)}$ (resp. $\overline{\pi}_{j,j'}^{(i+1)}$) is the probability that SA_{i-1} (resp. SA_{i+1}) is in the j state and SD_{i-1} (resp. SD_{i+1}) is in the j' state, ($j, j' \in \{1, 0\}$, where, $1 =$"*active*" and $0 =$"*pasive*");
- $\rho_{j,j'}^{(i-1)}(0)$ (resp. $\rho_{j,j'}^{(i+1)}(h_{i+1})$) is the probability that SA_{i-1} (resp. SA_{i+1}) is in the j state, and SD_{i-1} (resp. SD_{i+1}) is in the j' state and b_{i-1} is *empty* (resp. b_{i+1} is *full*);
- $f_{j,j'}^{(i-1)}(0)$ (resp. $f_{j,j'}^{(i+1)}(h_{i+1})$) is the probability density of the content of the downstream dipole buffer when SA_{i-1} (resp. SA_{i+1}) is in the j state and SD_{i-1} (resp. SD_{i+1}) is in the j' state and b_{i-1} is *empty* (resp. b_{i+1} is *full*);
- $\overline{\lambda}_A^{(i-1)}(j, j')$ (resp. $\overline{\lambda}_D^{(i+1)}(j, j')$) is the rate transition from j to j' states of SA_{i-1} (resp. SD_{i+1}).

We can distinguish three different ways in which the server SA_i can move from the active aggregate state to the passive one. The first mode is caused by an active change current state of SA_i, and the second and third mode is caused by upstream server SA_{i-1} of the dipole DP_{i-1} and an empty buffer b_{i-1}. In this case the average aggregate rate $\hat{\lambda}_A^{(i)}$ of transition from the active to the passive state is made up of three parts [13, 14] given by the expression (24):

$$\hat{\lambda}_A^{(i)} = \hat{\lambda}_{A,1}^{(i)} + \hat{\lambda}_{A,2}^{(i)} + \hat{\lambda}_{A,3}^{(i)}. \tag{24}$$

The first part corresponds to a change in active current state of SA_i, which occurs with the rate $\hat{\lambda}_{A,1}^{(i)} = \overline{\lambda}_1^{(i)}$. Secondly, SA_i cannot be active when upstream SA_{i-1} is passive and the buffer b_{i-1} is empty. The number of jumps of this type of events per unit of time is obtained from the upstream dipole DP_{i-1} as determined by the value $f_{0,1}^{(i-1)}(0)$. This value is multiplied by the speed $\overline{v}_2^{(i-1)}$ at which the SD_{i-1} consumes fluid from the buffer b_{i-1}. This fact is conditioned by the aggregate probability $\hat{\pi}_A^{(i-1)}$ that the upstream server SD_{i-1} is capable of producing, that is $\hat{\pi}_A^{(i-1)} = \overline{\pi}_{1,1}^{(i-1)} + \overline{\pi}_{0,1}^{(i-1)} - \rho_{0,1}^{(i-1)}(0)$, based on which we obtain:

$$\hat{\lambda}_{A,2}^{(i)} = f_{0,1}^{(i-1)}(0) \cdot \overline{v}_2^{(i-1)} / \hat{\pi}_A^{(i-1)}.$$

The last type of jump from the *active* (operational) state to the *passive* state occurs when the upstream buffer b_{i-1} is *empty* and the server SA_{i-1} is *active*. This case occur with

probability $\rho_{1,1}^{(i-1)}(0)$. If in this case the upstream server SA_{i-1} goes into the *passive* (non-operational) state, which happens with the average rate $\overline{\lambda}_2^{(i-1)}$, the considered server SA_i also goes into the *passive* state. This fact is conditioned by the probability that the upstream server SD_{i-1} can produce, that's how we get:

$$\hat{\lambda}_{A,3}^{(i)} = \rho_{0,1}^{(i-1)}(0) \cdot \overline{\lambda}_2^{(i-1)} / \hat{\pi}_A^{(i-1)}.$$

Similarly, to determine the *average delay* $1/\hat{\mu}_A^{(i-1)}$ of stay in the passive state of SD_{i-1}, we use the fact that a jump from the active to the passive state is determined by the probability $\overline{\lambda}_{A,1}^{(i)} / \hat{\lambda}_A^{(i)}$ of a change from the active state to the passive state and the probability $(\hat{\lambda}_{A,2}^{(i)} + \hat{\lambda}_{A,3}^{(i)}) / \hat{\lambda}_A^{(i)}$ of starvation. In the first case, we have an average wait time $1/\hat{\mu}_A^{(i)}$ in passive state and in the second case we get the average wait time $1/\overline{\lambda}_1^{(i-1)}$ in passive state of the upstream server SD_{i-1}. Thus, the estimated *average delay* $1/\hat{\mu}_A^{(i-1)}$ presence in the passive state of the upstream server SD_{i-1} is a weighted average for these two probabilities and it is given by the expression (25):

$$\frac{1}{\hat{\mu}_A^{(i-1)}} = \frac{\hat{\lambda}_{A,1}^{(i)}}{\hat{\lambda}_A^{(i)}} \cdot \frac{1}{\overline{\mu}_1^{(i)}} + \frac{\hat{\lambda}_{A,2}^{(i)} + \hat{\lambda}_{A,3}^{(i)}}{\hat{\lambda}_A^{(i)}} \cdot \frac{1}{\overline{\lambda}_1^{(i-1)}}. \tag{25}$$

The average aggregate speed $\hat{v}_A^{(i)}$ of data processing by SA_i in the active state is a weighted average of two possible speeds, being conditioned by the fact that SD_{i-1} produces (and thus SA_i is active) and the fact that the upstream buffer b_{i-1} is empty with probability $\rho_{1,1}^{(i-1)}(0) / \hat{\pi}_{A,2}^{(i-1)}$. In this case, the server SA_i must adjust speed to speed of SA_{i-1}, that produces speed $\hat{v}_A^{(i-1)}$. Also, with the complementary probability, the upstream server is capable of producing at maximum speed $\overline{v}_i$. Thus, we obtain $\hat{v}_A^{(i)}$:

$$\hat{v}_A^{(i)} = \overline{v}_i - (\overline{v}_i - \hat{v}_A^{(i-1)}) \cdot \rho_{1,1}^{(i-1)}(0) / \hat{\pi}_A^{(i-1)}. \tag{26}$$

Similarly, as for the server SA_i, we can divide in three parts the aggregate average rate transition from the active state to the passive state of the server SD_i we obtain $\hat{\lambda}_D^{(i)}$:

$$\hat{\lambda}_D^{(i)} = \hat{\lambda}_{D,1}^{(i)} + \hat{\lambda}_{D,2}^{(i)} + \hat{\lambda}_{D,3}^{(i)}. \tag{27}$$

The first part corresponds to a current change of the server SD_i from the active state to the passive one, which occurs with the rate $\hat{\lambda}_{D,1}^{(i)} = \overline{\lambda}_2^{(i)}$, and the second and third part are jumps caused by blocking this server when its downstream buffer b_{i+1} is *full*.

As the analysis follows along the same SCP, in the same way as for the server SA_i, there we will present only the expressions of the *jump aggregate rates* between states and of the respective aggregate average speed in this case for SD_i:

$$\hat{\lambda}_{D,1}^{(i)} = \overline{\lambda}_2^{(i)}, \quad \hat{\lambda}_{D,2}^{(i)} = f_{1,0}^{(i+1)}(h_{i+1}) \cdot \hat{v}_D^{(i+1)} / \hat{\pi}_D^{(i+1)},$$

$$\hat{\lambda}_{D,3}^{(i)} = \rho_{1,1}^{(i+1)}(h_{i+1}) \cdot \overline{\lambda}_2^{(i+1)}(j, j') / \hat{\pi}_D^{(i+1)},$$

$$\frac{1}{\hat{\mu}_D^{(i)}} = \frac{\hat{\lambda}_{D,1}^{(i)}}{\hat{\lambda}_D^{(i)}} \cdot \frac{1}{\overline{\mu}_2^{i+1}} + \frac{\hat{\lambda}_{D,2}^{(i)} + \hat{\lambda}_{D,3}^{(i)}}{\hat{\lambda}_D^{(i)}} \cdot \frac{1}{\overline{\lambda}_2^{(i+1)}}, \tag{28}$$

$\hat{v}_D^{(i)} = \overline{v}_{i+1} - (\overline{v}_{i+1} - \hat{v}_D^{(i+1)}) \cdot \rho_{1,1}^{(i+1)}(h_{i+1}) / \hat{\pi}_D^{(i+1)}$, where:

$$\hat{\pi}_D^{(i+1)} = \pi_{1,1}^{(i+1)} + \pi_{1,0}^{(i+1)} - \rho_{1,0}^{(i+1)}(h_{i+1}).$$

The aggregate quantitative parameters of each particular dipole thus determined are then used to evaluate the performance mesures of the entire analyzed $FSHPN$ model. For this, we present an algorithm in a fixed point iteration scheme for the analysis of a $FSHPN$, which is similar to the one in the papers [13, 14].

5.2. The fixed point iterative algorithm for the performance evaluation of $FSHPNs$

Based on the use of the method described in sections 3 and 4 to properly obtain the *average throughput* of and the average buffer level $\overline{x}_i$ estimation, modeled by SHPN, we apply the following ***fixed point iterative algorithm***:

Start. Step 0. *Initialization*: We initially assume that each dipole DP_i, $i = 1, \cdots, N-1$, is not affected by starvation or blocking due to upstream or downstream dipoles. The $\widetilde{\lambda}_{i,j}(M)$ and $\widetilde{v}_{i,l}$ of Sv_i, $i = 1, \cdots, N$ are set accordingly. Also, we set the initial value of the *iteration counter* $k = 0$.

Step 1. Using the PIPE 4.3 ToolKit [20], we calculate the stationary probabilities π_j of stay in the accessible marking M_j of the initial GSPN discrete part of the analyzed FSHPN model. For each dipole DP_i, $i = 1, 2, \cdots, N-1$ in the base of π_j we calculate the average rates $\overline{\lambda}_1^{(i)}$, $\overline{\lambda}_2^{(i)}$, $\overline{\mu}_1^{(i)}$, $\overline{\mu}_2^{(i)}$ of change of the current states and the average data processing speeds $\overline{v}_1^{(i)}, \overline{v}_2^{(i)}$. Depending on the relations between the values $\overline{v}_1^{(i)}$ and $\overline{v}_2^{(i)}$, based on the expressions (9) and (16) - (20) we calculate the values of the respective aggregate parameters of DP_i:

$$\gamma_k^i = \overline{\eta}_{v2}^{(i)} \text{ and } \hat{\lambda}_A^{(i)}, \ \hat{\lambda}_D^{(i)}, \ \hat{\mu}_A^{(i)}, \ \hat{\mu}_D^{(i)}, \ \hat{v}_A^{(i)}, \ \hat{v}_D^{(i)}.$$

Step 2. For each dipole DP_i, $i = 1, 2, \cdots, N-1$ we perform the following operations:

2.1) We increase the iteration counter by one, i.e. $k = k + 1$;

2.2) We set $\overline{\lambda}_1^{(i)} = \hat{\lambda}_A^{(i)}$, $\overline{\lambda}_2^{(i)} = \hat{\lambda}_D^{(i)}$, $\overline{\mu}_1^{(i)} = \overline{\mu}_A^{(i)}$, $\overline{\mu}_2^{(i+1)} = \hat{\mu}_D^{(i)}$, $\overline{v}_1^{(i)} = \overline{v}_A^{(i)}$ and $\overline{v}_2^{(i)} = \hat{v}_D^{(i)}$;

2.3) Depending on the relations between the values $\overline{v}_1^{(i)}$ and $\overline{v}_2^{(i)}$ for these new parameters values of dipole DP_i, we calculate the stationary probabilities $\pi_{j,j'}^{(i)}$, the boundary probabilities $\rho_{j,j'}^{(i)}(0)$ and $\rho_{j,j'}^{(i)}(h_i)$, the probability density function $f_{j,j'}^{(i)}(x_i)$ of the buffer b_i content and the *average throughput* $\gamma_k^i = \overline{\eta}_{v2}^{(i)}$ estimated at the k iteration, based on which we calculate: $\hat{\lambda}_A^{(i)}$, $\hat{\lambda}_D^{(i)}$, $\hat{\mu}_A^{(i)}$, $\hat{\mu}_D^{(i)}$, $\hat{v}_A^{(i)}$, $\hat{v}_D^{(i)}$;

2.4) If, $i < N-1$we adjust the aggregate rates $\hat{\lambda}_A^{(i+1)}$ and aggregate speeds $\hat{v}_A^{(i+1)}$ of the down-stream dipole DP_{i+1}, using the respective expressions in subsection IV;

2.5) If, $i > 1$ we adjust the parameters $\hat{\lambda}_D^{(i-1)}$ and speed $\bar{v}_D^{(i-1)}$ of the upstream dipole DP_{i+1}, using the respective expressions in subsection IV.

Step 3. *Convergence check*. Repeat Step 2 until we get convergence for all estimats productivities $\gamma_k^{(i)}$ of $FSHPN$ model. That if $\min_{\forall i}\left((|\gamma_k^{(i)} - \gamma_{k-1}^{(i)}|)/\gamma_k^{(i)}\right) > \varepsilon$ for a very small speci-fied precision value ε, we get to do another iteration; otherwise we go to *step* 4.

Step 4. For each dipole DP_i, $i = 1,2,\cdots,N-1$, based on the quantitative parameters being obtained at the last iteration, we calculate, according to the expression (8), the average fluid level $\bar{x}_i$ in the buffer b_i, then we ***stop*** the calculations and show the specified results. **Stop.**

To validate the developed method in this paper, a large set of tests was used in which the *average throughput* of the $FSHPN1$ model and the average content of the respective buffers were approximated with those obtained by simulation methods with discrete events using NS-2 simulator [23]. It was found that the values $\gamma_k^{(i)}$ of all dipoles converge to the same values for which the maximum error of the developed method while estimating the average *throughput* of the system is less than 2.60%, corresponding to the system with six pipe-line dipoles DP_i, and $1 \le h_i \le 10$ of buffers. Concerning the average buffer level $\bar{x}_i$ estimation, the maximum error is below 3%. The accuracy of the insensitive method appears to the number of buffers and the number of timed transitions per servers Sv_i.

Conclusions

In this paper we present an approximated main-value analysis method of stochastic hybrid Petri nets (SHPN) models with fuzzy parameters, called FSHPN, for performance evaluation of continuous data transmission CSN virtual channels. The method is based on the main-value analytical solution of one buffer finite FSHPN sub-models, also referred dipoles as building blocks. We develop an iterative fixed point algorithm to accurately estimate performance measures of buffer pipe-line FSHPN models such as throughput and mean buffer contents. The approach is general and it can be applied to several pipe-line dipoles without mining the accuracy in the estimation. The accuracy of the proposed method has been validated by numerical simulation experiments. The use of a large set of numerical tests shows that performance evaluation result of FSHPN models by using the proposed method is quite close to those obtained by simulation, and proposed method is less time-consuming. Further research can also include the adaption of this method to $SHPN$ models with intuitionistic fuzzy parameters and/or more buffers are incident forward/backward to the continuous transitions, i. e. $|{}^\bullet u_i| > 1$and/or $|u_i^\bullet| > 1$. Also, this approach can be further generalized to systems performance analysis from domains with dynamically reconfigurable behaviour characteristics that are conditioned by events specified at the design stage.

Conflicts of Interest: The authors declare no conflict of interest.

References

1. Suarez F. J., Nuno P., Granda J. C., Garcia D. F. *computer networks performance modeling and simulation*. [online]. In book: Modeling and simulation of computer networks and systems - methodologies and applications, chapter 7, 2015, pp.187-223. [accessed 05.02.2020]. available AT: https://www.researchgate.net/publication/282076891_computer_networks_performance_modeling_and_simulation
2. Harchol-Balter M. *Performance modeling and design of computer systems: queueing theory in action*. [online]. Carnegie Mellon University, Pennsylvania, 2013. -574 p. [accessed 06.02.2020]. available at: https://mecsenotes.weebly.com/uploads/4/7/6/5/47654023/1107027500.pdf57
3. Augustin T., Miranda E., Vejnarova J. Imprecise probability models and their applications. In: *International Journal of Approximate Reasoning*, 50(4), 2009, pp. 581 – 582.
4. Murata T. Petri Nets: Properties, Analysis and Applications. *Proceedings of IEEE*, vol.77, no.4, 1989, pp.541-580.
5. Chiola, G., Ajmone- Marsan, M., Balbo, G., Conte, G. Generalized stochastic Petri nets: A definition at the net level and its implications. In: *IEEE Transactions on Software Engineering*, 1993, 19 (2), pp. 89-107.
6. Ciardo G., Trivedi, K. S. A Decomposition Approach for Stochastic Reward Net Models. In: Performance Evaluation 18 (1),1993, pp. 37–59.
7. Horton G., Kulkarni V. G., Nicol D. M., Trivedi K. S. Fluid stochastic Petri nets: Theory, application, and solution techniques. *Eur. J. Op. Res.* 105(1), 1998, pp. 184–201.
8. Guţuleac E. Descriptive compositional HSPN modeling of computer systems. In: *Annals of the Craiova University*, *Series: Atomation, Computers, Electronics and Mechatronics, România*, 2006, Vol. 3 (30), no.2, pp.82-87.
9. Guţuleac E. Performance evaluation of computer systems with stochastic Petri nets (in Romanian). Ed.: Tehnica-Info, Chişinău, 2004. - 276 p.
10. Tüysüz F., Kahraman C. Modeling a flexible manufacturing cell using stochastic Petri nets with fuzzy parameters. [Online]. In: Expert Systems with Applications 37, 2010, pp. 3910–3920. [Accessed 11.05.2018]. Available at: https://www.researchgate.net/publication/287993951
11. Tavassoli S., Shahpar F., Hejazi T. H. A fuzzy approach to reliability analysis. In: *Journal of Industrial Engineering and Management Studies*, Vol. 4, No. 1, 2017, pp. 55-68.
12. Gribaudo, M., Sereno, M. Simulation of Fluid Stochastic Petri Nets. In: Proc. 8th Int. Symposium on Modeling, Analysis and Simulation of Computer and Telecommunication Systems. San Francisco, 2000, pp. 231-239.
13. Bierbooms R., Adan I., Vuuren M. Approximate performance analysis of production lines with continuous material flows and finite buffers, In: *Stochastic Models*, 29, 2013, pp. 1–30.
14. Colledani M., Gershwin S. A. Decomposition method for approximate evaluation of continuous flow multi-stage lines with general Markovian machines. In: Annals Oper. Res., 209, pp. 5–40, 2013.
15. Desmita Z., Mashadi A. Alternative Multiplying Triangular Fuzzy Number and Applied in Fully Fuzzy Linear System. In: *American Scientific Research Journal for Engineering, Technology, and Sciences***,** Vol. 56, No 1, 2019, pp. 113-123.
16. Alzeidia, N., Khonsarib, A., Ould-Khaouaa, M., Mackenziea. L. A new approach to model virtual channels in interconnection networks. In: *Journal of Computer and System Sciences*, 73, 2007, pp. 1121–1130.
17. Unterhuber P. et all. *A survey of channel measurements and models for current and future railway communication systems*. [online]. in: Mobile information systems, vol. 2016, article ID 7308604, pp. 1-14. [accessed 11.05.2018]. available at: http://downloads.hindawi.com/journals/misy/2016/7308604.pdf
18. Khuwaja A. A., Chen Y., Zhao N., Alouini M.-S., Dobbins, P. A survey of channel modeling for UAV communications. In: *IEEE Communications Surveys & Tutorials*, vol. 20, no. 4, 2018, pp. 2804 – 2821.
19. Guţuleac E., Boşneaga C., Reilean A. VPNP-Software tool for modeling and performance evaluation using generalized stochastic Petri nets. In: *Proceedings of 6-th International Conference on D&AS-2002*, Suceava, România, 2002, pp. 243-248.
20. Petri nets world - Petri nets tools database. *http://www.informatik.uni-hamburg.de/TGI/PetriNets/tools/quick.html*
21. Mosleh M., Abbasbandy S., Otadi M. A method for solving fully fuzzy linear system. In: Mathematics Scientic Journal, Vol. 7, No. 2, 2011, pp. 55-66.
22. Radhakrishnan S., Gajivaradhan P., Govindarajan R. A New and Simple Method of Solving Fully Fuzzy Linear System. In: *Annals of Pure and Applied Mathematics*, Vol. 8, No. 2, 2014, pp. 193-199.
23. NS-2 simulator. [Online]. [Accessed 19.02.2020]. Available at: http://ns2projects.org/ns2-simulator-free-download/